Exploring chemical space in covalent and competitive glycosidase inhibitor design

Chen, Y.

4

Synthesis and Biochemical Evaluation of Bifunctional Cyclophellitol Aziridines as Selective GBA Inhibitors and Activity-Based Probes

Part of this chapter is published as:

Rhianna J. Rowland,[*] Yurong Chen,[*] Imogen Breen, Liang Wu, Wendy A. Offen, Thomas J. Beenakker, Qin Su, Adrianus M. C. H. van den Nieuwendijk, Johannes M. F. G. Aerts, Marta Artola, Herman S. Overkleeft and Gideon J. Davies, *Chem. Eur. J.* **2021**, *27*, 1–13.

4.1 Introduction

Glucocerebrosidase (acid glucosylceramidase, GCase, GBA, EC 3.2.1.45), belonging to the glycoside hydrolase (GH) 30 family (www.cazy.org),[1] is a lysosomal retaining β-glucosidase. GBA is primarily responsible for catalyzing the degradation, in lysosomes, of glucosylceramide (GlcCer) by hydrolytic cleavage of the β-glucose moiety from the aglycon to yield free ceramide and glucose with net retention of β-anomeric configuration,[2–4] through a two-step Koshland double displacement mechanism (Figure 4.1). Inherited deficiency in GBA causes the most common lysosomal storage disorder, Gaucher disease (GD), which is primarily characterized by the cellular accumulation of GlcCer, and its deacylated derivative glucosylsphingosine (GlcSph).[2,5,6] The multisystemic storage of these glycolipids leads to the clinical symptoms of GD, which can vary considerably in frequency and severity. Clinical manifestation of GD type 1 and GD type 2 commonly include skeletal disease and visceral disease affecting the spleen, kidneys, liver and heart.[7–10] In more severe cases (GD type 3), neurological disorders also arise due to GlcCer deposition in the brain.[11,12] Moreover, mutations in the gene coding for GBA have recently been identified as the highest known genetic risk factor for Parkinson's disease (PD).[13–15] Thanks to the clinical importance of GBA in both GD and PD, it is one of the most widely studied human glucosidase with relentless interest in developing novel chaperones,[16–19] inhibitors,[20–22] and activity-based probes (ABPs)[23–25] to study this enzyme in disease pathogenesis, diagnosis and treatment.

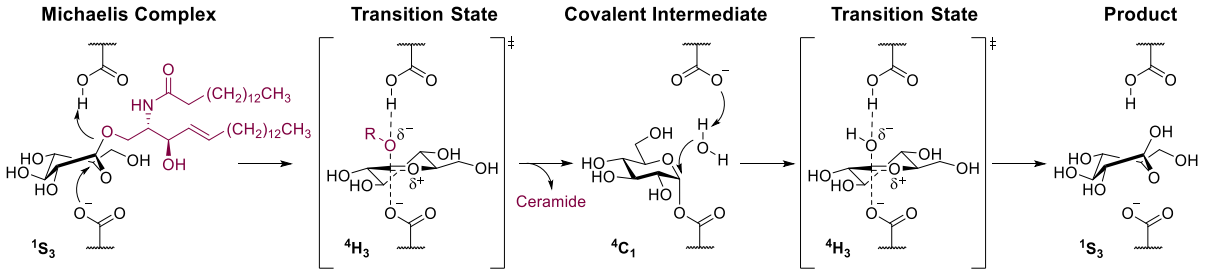

Figure 4.1. Glucocerebrosidase (GBA) catalyzes the hydrolysis of glucosylceramide in a two-step double displacement mechanism to yield glucose and ceramide.

Cyclophellitol **1**, a natural product originally isolated from *Phellinus sp.*, is a potent irreversible inhibitor of retaining β-glucosidases, and inactivates GBA and GBA2 with merely equal efficiency.[26] Previous studies have shown that functionalization at the C6 position of cyclophellitol (cyclophellitol numbering is depicted in Figure 4.2) with a BODIPY reporter group yielded highly potent and very specific activity-based probes (ABPs) to monitor GBA activity *in vitro*, *in situ*, and *in vivo*,[23,27] with potential applications in diagnostics and

therapeutic evaluation. More recently, this methodology was further extended with the design of a C6-Cy5 tagged cyclophellitol ABP **3** and C6-biphenyl/adamantanyl substituted cyclophellitol derivatives **4** and **5**.[22] Both compounds **4** and **5** proved to be very potent and selective GBA inhibitors *in vitro* and *in vivo*, and are suitable for generating neuropathic Gaucher zebrafish models. In the studies on cyclophellitol analogues, substitution of the epoxide oxygen for nitrogen led to the synthesis of cyclophellitol aziridine **2**,[28] which inhibits retaining β-glucosidases with equal or slightly higher potency than the parent cyclophellitol **1**. One route to modify cyclophellitol aziridines and facilitate their conversion to ABPs is functionalization of the aziridine nitrogen. Consequently, installation of reporter moieties (BODIPY, Cy5 or biotin) at the aziridine nitrogen through *N*-acylation[24] or *N*-alkylation[25] yielded broad spectrum retaining β-glucosidase ABPs, which can efficiently label the four human retaining β-glucosidases, GBA, GBA2, GBA3 and lactase-phlorizin hydrolase (LPH).

GBA is notable for its tolerance, indeed preference, for C6-substituted reagents which exhibit increased specificity for GBA over other β-glucosidases (GBA2, GBA3 and LPH), [22,23] while it also favors iminosugar inhibitors[29,30] and cyclophellitol aziridines[24,25] extended at the aziridine nitrogen position. These preferences of GBA suggested that binding of the C6-substituent and aziridine *N*-functionalization may reflect the enzyme's specificity for a lipid substrate with two alkyl tails. It would be of interest to investigate whether a new generation of bi-functional cyclophellitol aziridines, which are functionalized at both the C6-position and the aziridine nitrogen, may exhibit further improvements in potency and selectivity for GBA. In this chapter, the synthesis of a C6-Cy5 tagged *N*-octyl-cyclophellitol aziridine **7** is described, and its GBA activity and selectivity are compared to Cy5 tagged cyclophellitol epoxide **3** and Cy5 cyclophellitol aziridine **6**. Moreover, and in line with previous findings that C6-biphenyl/adamantanyl substituted cyclophellitols are very potent and selective GBA inhibitors, the corresponding bifunctional cyclophellitol aziridine inhibitors **8** and **9** were synthesized, and their *in vitro* activity and selectivity toward GBA evaluated as well.

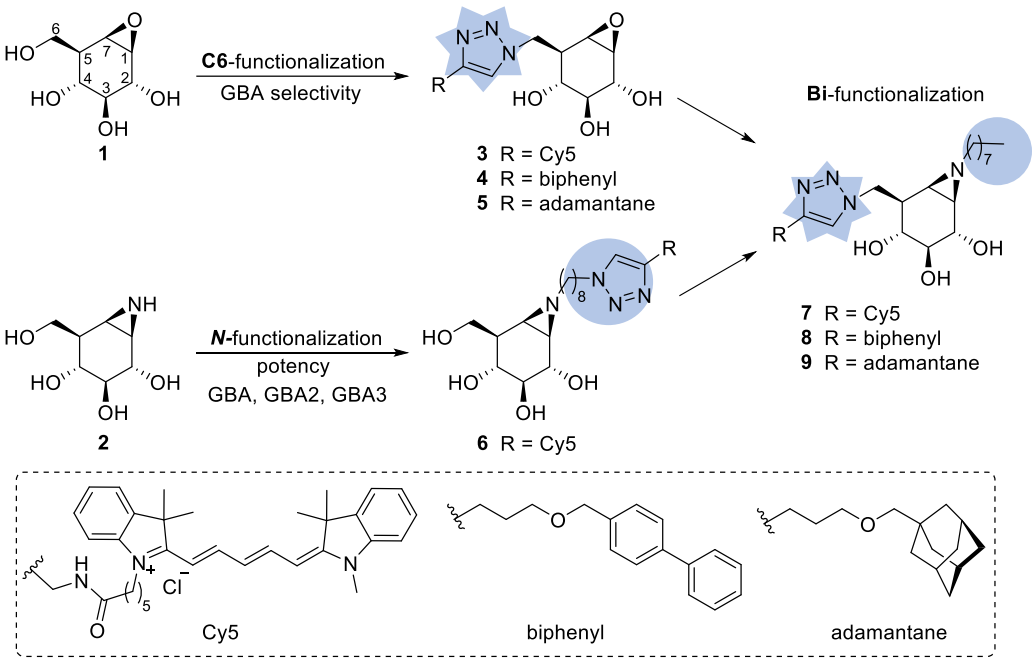

Figure 4.2. Structures of covalent and irreversible retaining β-glucosidase inhibitors and ABPs described in this chapter: cyclophellitol **1** and its C6-functionalized derivatives **3-5**; cyclophellitol aziridine **2** and its *N*-functionalized ABP **6** and bi-functionalized derivatives **7-9**.

4.2 Results and discussion

4.2.1 Synthesis of bi-functionalized cyclophellitol aziridine ABPs and inhibitors

It was envisioned that target cyclophellitol aziridines **7-9** could be obtained from azide **11** via click-chemistry. To gain access to azide **11** (Scheme 4.1), compound **2** was synthesized according to the literature procedures.[28] Reaction of aziridine **2** with 1-iodooctane at 55 °C for prolonged reaction times resulted in isolation of **10** in 39% yield. Introduction of an azido functionality at C6 position was first performed via a two-step procedure. While tosylation of the primary alcohol with an excess of tosyl chloride (6.0 eq.) in the presence of Et_3N (7.2 eq.) gave no reaction at room temperature, heating the reaction to 40 °C resulted in the formation of intermediate **S1** after prolonged reaction times. After work-up, tosylate **S1** was directly reacted with excess sodium azide (20 eq.). However, no conversion of the starting material was observed at 50 °C even after 2 days and increasing the temperature to 80 °C mainly resulted in nucleophilic opening of the aziridine. Other attempts to directly introduce the azido group in one step using diphenylphosphoryl azide (DPPA) in the presence diisopropylazodicarboxylate (DIAD) and triphenylphosphine (Ph_3P)[31–33] were unproductive as well, possibly due to the low reactivity of the unprotected aziridine. Alternatively, the primary alcohol in **10** could be alkylated with an 8-azidooctyl trifluoromethanesulfonate linker, giving compound **12** in low

yield. The azide handle could then be functionalized with a Cy5 dye by click-chemistry to afford ABP **13** after HPLC purification. Although not the final target, ABP **13** can also be studied as a bifunctional probe of GBA.

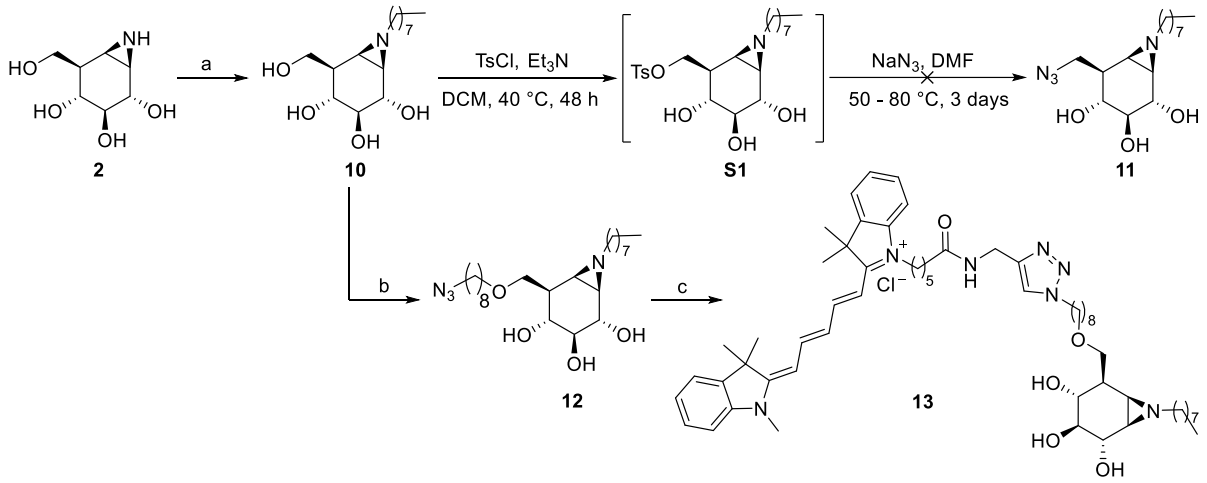

Scheme 4.1. Synthesis of ABP **13**. Reagents and conditions: a) 1-iodooctane, K_2CO_3, DMF, 55 °C, 48 h, 39%; b) 8-azidooctyl trifluoromethanesulfonate, DIPEA, DCM, rt, 4 days, 11%; c) Cy5-alkyne, $CuSO_4$, NaAsc, DMF, rt, 24 h, 25%.

In another attempt to obtain the target C6-azido *N*-octyl aziridine **11**, a new synthetic route following a key 2-naphthylmethyl ether (Nap) protecting group strategy was developed (Scheme 4.2). Briefly, starting intermediate **14** was synthesized in nine steps from D-xylose based on chemistry developed by Madsen and co-workers.[34,35] Standard benzyl deprotection conditions (i.e. Birch reduction or palladium catalyzed hydrogenation) were not compatible with the required azide functionality and electrophilic aziridine, therefore, debenzylation of **14** with boron trichloride (BCl_3) was performed at an early stage, followed by selective tritylation of the primary alcohol affording intermediate **15**. The remaining secondary alcohols were protected as Nap ethers followed by detritylation of the primary alcohol to afford **16**. Treatment of **16** with trichloroacetonitrile yielded a primary imidate intermediate **S2**, which was found to be unstable and partly decomposed during a purification attempt by column chromatography, forming a less polar impurity which was eluted out together with the product. The mixture containing **S2** was directly treated with *N*- iodosuccinimide (NIS) which resulted in the isolation of cyclic imidate **17** in a moderate yield (40%). Hydrolysis of **17** under acidic conditions and subsequent treatment of the resulting ammonium salt with excess base resulted in intramolecular iodine displacement to form a free aziridine, which was then alkylated with an octyl linker to give compound **18**. Tosylation of the primary alcohol using Et_3N as the single base proved to be sluggish, therefore the combination of Et_3N (2.0 eq.) and *N*-methyl imidazole

(7.0 eq.) was employed, allowing complete tosylation of **18** after 28 hours as indicated by TLC-analysis. After work-up, the resulting crude tosylate was reacted with an excess of sodium azide (10.0 eq.) under gentle heating for prolonged reaction times (40 h), resulting in **19** in 68% yield after two steps. The naphthylmethyl ethers were then removed by DDQ to afford compound **11**, which was finally functionalized with appropriate alkynes using click-chemistry to give ABP **7** and inhibitors **8**-**9** after HPLC purification (Scheme 4.2).

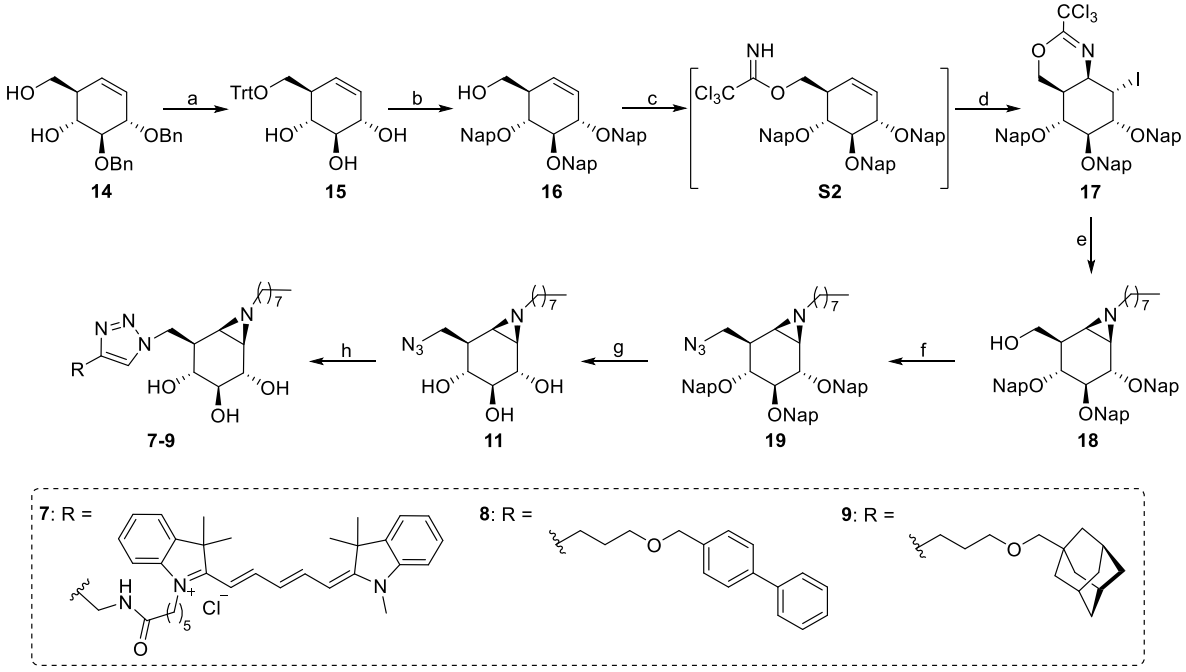

Scheme 4.2. Synthesis of ABP **7** and inhibitors **8**-**9**. Reagents and conditions: a) *i*) BCl_3, DCM, -78 °C, 2 h; *ii*) TrCl, Et_3N, DMAP, DMF, rt, 19 h, 30% over two steps; b) *i*) NapBr, NaH, TBAI, DMF, 0 °C – rt, 5 h; *ii*) TsOH, DCM/MeOH (1/1), rt, overnight, 73% over two steps; c) Cl_3CCN, DBU, DCM, rt, overnight; d) NIS, $CHCl_3$, rt, 17 h, 40% over two steps; e) *i*) HCl, DCM/MeOH (1/1), rt, overnight, then Amberlite IRA-67, 20 h; *ii*) 1-iodooctane, K_2CO_3, DMF, 80 °C, 16 h, 35% over two steps; f) *i*) TsCl, Et_3N, *N*-methyl imidazole, DCM, rt, 28 h; *ii*) NaN_3, DMF, 50 °C, 40 h, 68% over two steps; g) DDQ, DCM/H_2O (10/1), rt, 24 h, 66%; h) Cy5-alkyne, $CuSO_4$, NaAsc, DMF, rt, overnight, 30%.

4.2.2 Structural analysis of the ABP 7-enzyme complex

To investigate the accommodation of the two functionalities of ABP **7** by recombinant human GBA (rhGBA, produced in an insect-baculovirus expression vector system (BEVS)[37]), a co-crystal structure in complex with bi-functional ABP **7** was obtained at 1.80 Å resolution, demonstrating covalent binding of the cyclophellitol aziridine to the catalytic nucleophile of GBA (Figure 4.3). Specifically, the reacted cyclophellitol adopts the expected $^4C_1$ chair conformation, with a covalent bond length of 1.47 Å to Glu340. Furthermore, unambiguous electron density for the ring opened *N*-alkyl aziridine warhead was observed, allowing the first

5 carbons of the *N*-octyl chain to be modelled. This was sufficient to establish binding of the *N*-alkyl chain to the narrow active site channel formed by Gln284, Tyr313, Lys346 and Trp348. In fact, the *N*-alkyl chain of ABP **7** extends through this pocket towards the surface of the protein, which may provide some indication into the binding of the fatty acid portion of the natural GlcCer substrate which is thought to project out from the protein and interact with the lipid bilayer.[36] Unfortunately, whilst sufficient electron density for the O6-triazole linker and subsequent amide group was observed, the Cy5 tag could not be modelled. Nevertheless, the O6-triazole linker was found to bind in the hydrophobic cavity formed by Trp348, Phe246 and Tyr313, which was reported previously to accommodate the triazole linker of ABP **3**.[22] Additionally, this binding cavity extends towards the broader hydrophobic allosteric site at the dimer interface where a previously reported C6-BODIPY tag was shown to bind.[23]

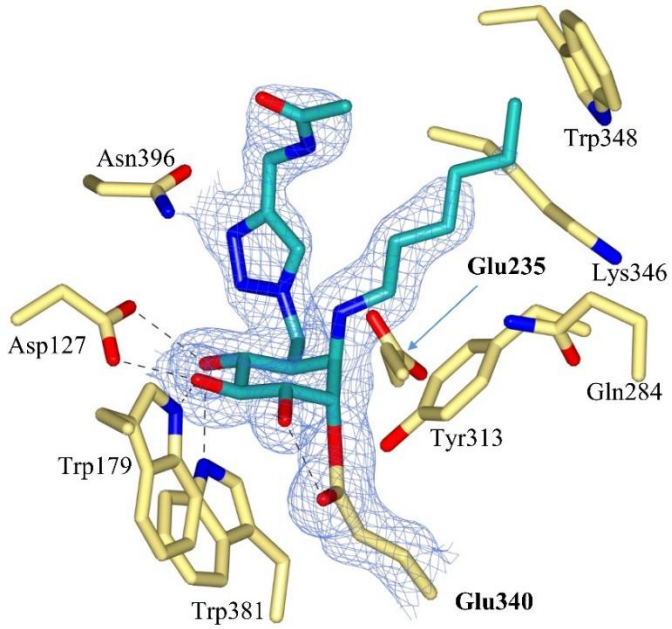

Figure 4.3. Observed electron density for ABP **7** bound covalently to the catalytic nucleophile (Glu340) of rhGBA by trans-diaxial ring opening of the *N*-alkyl aziridine warhead. Maximum-likelihood/σA weighted ($2F_o$-F_c) electron density map contoured to 1.0 σ (a = 1.31 $e^-/Å^3$).

4.2.3 Fluorescent labeling of rhGBA with ABP 3 and ABP 7

Activity-based labeling of rhGBA (produced in BEVS) with bi-functional ABP **7** was performed and compared to labeling by its C6-mono-functionalized epoxide derivative ABP **3**. Firstly, in solution labeling of excess rhGBA (200 nM) was performed in the presence of decreasing ABP concentrations (150-0.001 nM), demonstrating clear concentration dependent labeling with a gel-detection limit of 1 nM for ABP **7** and 0.1 nM for ABP **3** (Figure 4.4A). Secondly, labeling assays in which ABP **7** and ABP **3** (150 nM) were incubated with decreasing

rhGBA concentrations (500-0.01 nM) were performed to further demonstrate the concentration dependent labeling down to 1 nM rhGBA with ABP **7** and 0.1 nM rhGBA with ABP **3** (Figure 4.4B). Additionally, denaturing the enzyme prior to probe incubation totally abrogated labeling in all assays, indicating that labeling is activity-based. These in gel detection limits are concordant across both assays and demonstrate that ABP **3** exhibits ~ 10-fold higher potency than **7**.

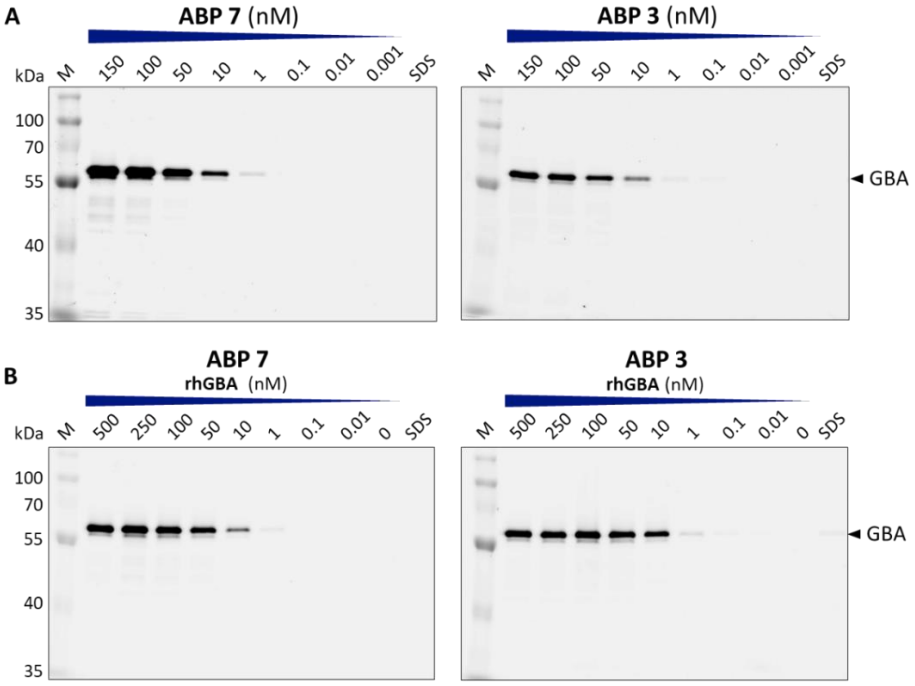

Figure 4.4. A) Labeling of rhGBA (200 nM) with decreasing concentrations (150-0.001 nM) of ABP **3** or ABP **7** at 37 °C for 30 mins followed by SDS-PAGE separation. B) Incubation of ABP **3** or ABP **7** (150 nM) with decreasing concentrations of rhGBA (500-0.01 nM) followed by SDS-PAGE analysis. Fluorescently labeled rhGBA visualized by Cy5 fluorescent readout. SDS = denatured protein sample.

4.2.4 *In vitro* activity and selectivity of bi-functionalized cyclophellitol aziridines

To further investigate the potency and selectivity of the newly synthesized ABPs (**7** and **13**) and inhibitors (**8** and **9**), *in vitro* activity assays against GBA and two related β- and α-glucosidases (GBA2 and GAA) were performed and compared to known C6-mono-functionalized epoxide derivatives **3**-**5**.

Compounds **7**, **8**, **9** and **13** were pre-incubated with recombinant human GBA (rhGBA, Imiglucerase), human GBA2 (from lysates of GBA2 overexpressed cells) and recombinant human GAA (rhGAA, Myozyme) for 3 hours followed by enzymatic activity measurement using 4-methylumbelliferyl-β- and α-glucosides as fluorogenic substrates. As shown in Table

4.1, ABP **13** proved to be a nanomolar inhibitor of rhGBA (with an apparent IC_{50} value of 3.4 nM), which was 15-fold more potent than ABP **7** (with an apparent IC_{50} value of 53.1 nM). Both compounds **7** and **13** were rather inactive towards GBA2 and GAA (apparent IC_{50} values >10 μM), thus exhibiting comparable selective inhibition of GBA (IC_{50} ratio $>10^3$ for both GBA2/GBA and GAA/GBA) as reported previously for ABP **3**.[22] Inhibitors **8** and **9** had *in vitro* IC_{50} values of 10 to 13 nM towards rhGBA, and are thus 10- to 13-times less potent than their epoxide analogues **4** or **5** (apparent IC_{50} values around 1.0 nM). Similar to ABP **7** and **13**, both compounds **8** and **9** proved inactive to GBA2 and GAA, exhibiting IC_{50} ratio of > 10^4 for both GBA2/GBA and GAA/GBA.

Table 4.1. Apparent IC_{50} values for *in vitro* inhibition of rhGBA, rhGAA and GBA2 from overexpressed cell lysates by compounds 7, 8, 9 and 13. Error ranges depict standard deviations from technical duplicates.

***In vitro* IC_{50} (nM)**	**ABP 3**	**4**	**5**	**ABP 13**	**ABP 7**	**8**	**9**
rhGBA	3.20 ± 0.17[a]	1.06 ± 0.19 [a]	0.96 ± 0.17 [a]	3.35 ± 0.75	53.06 ± 2.65	13.35 ± 1.24	9.63 ± 0.01
GBA2 (HEK293T lysate)	412 x 10^3 ± 10.1 x 10^3 [a]	> 10^5 [a]	> 10^5 [a]	23.3 x 10^3 ± 0.13 x 10^3	> 10^5	> 10^5	> 10^5
rhGAA	> 10^5 [a]	> 10^5 [a]	> 10^5 [a]	> 10^5	> 10^5	> 10^5	> 10^5

[a]IC_{50} values from ref 22.

Next, the labeling efficiency and selectivity of ABPs **3**, **7** and **13** towards GBA in mouse brain lysate were evaluated at pH 5.2 (containing 0.2% taurocholate and 0.1% Triton-100) and pH 5.8 as these are the respective optimal conditions for GBA and GBA2 activities (Figure 4.5). As expected, ABPs **3**, **7** and **13** selectively labeled GBA in a concentration-dependent manner under pH 5.2 (upper panels), all with significant labeling observed at 10 nM of ABP. Under pH 5.8 (lower panels), the labeling efficiency of all three ABPs towards GBA decreased and significant labeling can only be observed at 1 μM (ABPs **7** and **13**) and 300 nM (ABP **3**). Importantly, no labeling of GBA2 was observed up to 1 μM, showing good GBA selectivity. For comparison, broad-spectrum β-glucosidase ABP **6** efficiently labeled both GBA and GBA2 at 100 nM under both pH conditions.

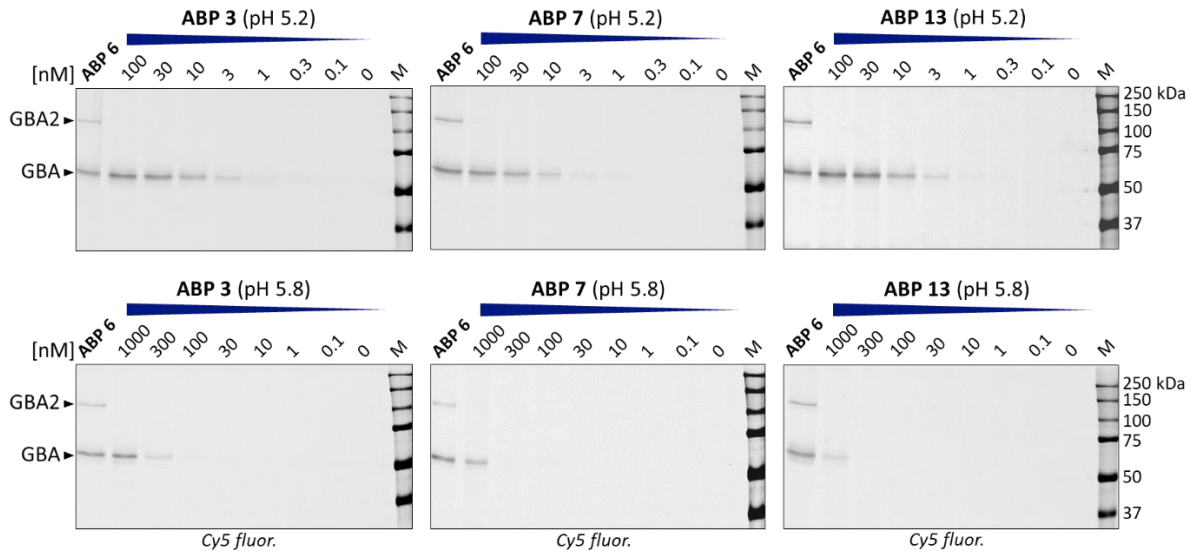

Figure 4.5. Fluorescent labeling of mouse brain lysate (25 µg total protein) with different concentrations of ABPs **3**, **7** and **13** at pH 5.2 (upper panels) or pH 5.8 (lower panels) after incubation for 30 min at 37 °C. Labeling by broad-spectrum β-glucosidase ABP **6** is shown for comparison (100 nM, pH 5.2 or pH 5.8, 30 min, 37 °C).

In addition to these studies, competitive ABPP experiments were performed (Figure 4.6). In this experiment, mouse brain lysates were pre-incubated with different concentrations of inhibitors **8** or **9**, followed by labeling of the residual active enzymes with 50 nM of broad-spectrum ABP **6**. Both compounds **8** and **9** could selectively inhibit GBA in a concentration-dependent manner in the range of 10–1 µM, although full labeling competition was not achieved below 10 µM. In line with the ABP 7 analogue, neither **8** nor **9** showed competition of GBA2 labeling even at the highest concentration applied (10 µM), demonstrating again that functionalization at C6 is detrimental for GBA2 binding.

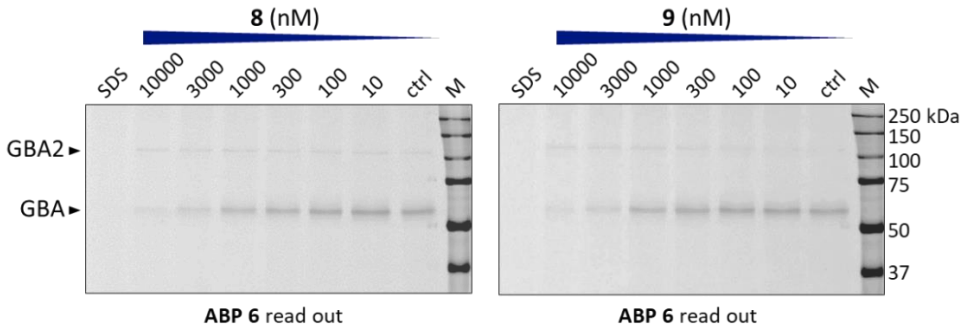

Figure 4.6. Competitive ABPP of mouse brain lysates with **8** and **9**. The sample (25 µg total protein) was pre-incubated with **8** or **9** at different concentrations (60 min, 37 °C, pH 5.2), followed by labeling with 50 nM of ABP **6** (30 min, 37 °C, pH 5.2).

4.2.5 *In situ* labeling of GBA and GBA2 in living cells by ABPs 3, 6 and 7

The selectivity of bi-functionalized ABP **7** towards GBA over GBA2 was further evaluated by *in situ* labeling of living cells and compared to that of broad-spectrum ABP **6** and C6-mono-functionalized epoxide ABP **3**. HEK293T cells containing endogenous GBA and overexpressed GBA2 were treated with the ABPs at different concentrations (1-1,000 nM) for 24 hr. Cells were then washed, lysed and visualized by SDS-PAGE gel-based fluorescence (Figure 4.7). Treatment with broad spectrum ABP **6** resulted in unbiased labeling of GBA and GBA2 at 10 nM, with labeling of both enzymes reaching saturation at 100 nM after 24 hours incubation. In comparison, selective labeling of GBA in ABP **7** treated cells was observed at 10 nM, with some GBA2 labeling observed at higher probe concentrations (100 nM). More selective labeling of GBA was achieved with ABP **3**, which did not label GBA2 even at the highest concentration of probe applied (1 µM).

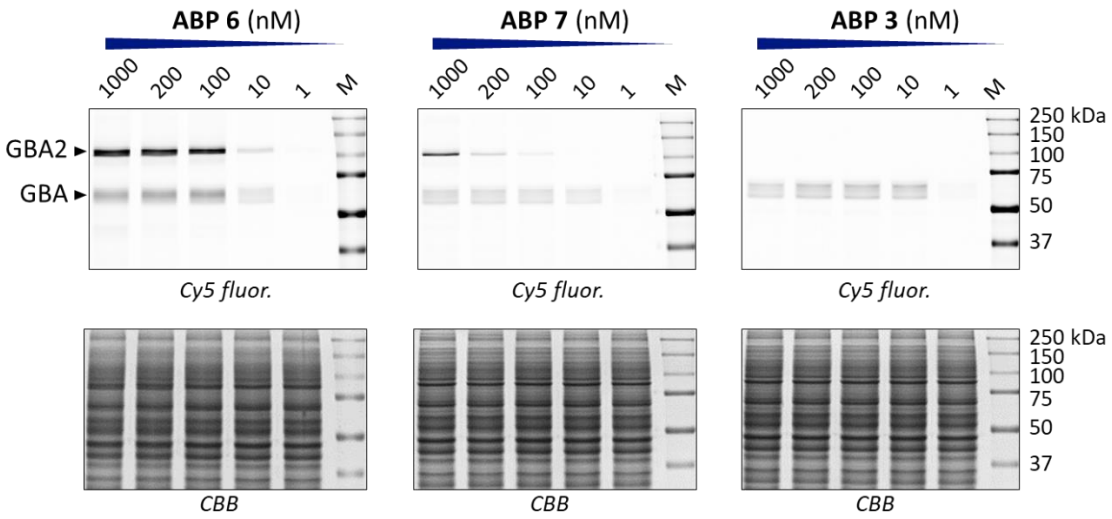

Figure 4.7. *In situ* labeling of GBA and GBA2 in HEK293T cells with ABPs **3**, **6** and **7** at varying concentrations at 37 °C for 24 h, followed by SDS-PAGE separation (top panels). *CBB*, Coomassie Brilliant Blue staining (bottom panels).

4.3 Conclusion

To summarize, this chapter describes the synthesis of a panel of bi-functional cyclophellitol aziridine ABPs and inhibitors for human β-glucocerebrosidase (GBA) with supportive structural analysis and ABPP studies. The X-ray structure of rhGBA in complex with ABP **7** not only demonstrates the mechanism-based mode of action of the compound as a covalent inactivator, but also highlights the binding of C6 and aziridine nitrogen substituents in two distinct active site clefts. Whilst it was structurally validated that the C6- and aziridine

functionalities are well accommodated in two binding cavities, these bi-functional ABPs and inhibitors showed no further improvement in potency or selectivity over their C6-mono-functionalized epoxide counterparts. Nevertheless, this work exemplifies the complexity of ABP development and these bi-functional compounds remain nanomolar inhibitors of GBA which may serve useful in the study of GBA in relation to Gaucher disease and inform the design of next-generation inhibitors and probes through modification of both the C6- and aziridine nitrogen substituents.

4.4 Acknowledgements

Rhianna Rowland and Gideon Davies from University of York, UK are kindly acknowledged for rhGBA (produced in BEVS) labeling experiments and crystallographic studies. Qin Su is acknowledged for his help with IC_{50} and *in situ* labeling experiments.

4.5 Experimental methods

4.5.1 Biochemical experiments

Materials

Recombinant human GBA (rhGBA, imiglucerase, Cerezyme®) and GAA (rhGAA, alglucosidase alfa, Myozyme) were obtained from Sanofi Genzyme (Cambridge, MA, USA). HEK293T (CRL-3216) cell lines were purchased from ATCC (Manassas, VA, USA). Cell lines were cultured in DMEM medium (Sigma-Aldrich, St. Lois, MO, USA), supplied with 10% (v/v) FCS, 0.1% (w/v) penicillin/streptomycin and 1% (v/v) Glutamax, under 5% CO_2 at 37°C. The generation of HEK293T cells overexpressing GBA2[38] and the preparation of cellular homogenates[22] were performed as previously described. Mouse tissue were isolated according to guidelines approved by the ethical committee of Leiden University (DEC#13191). All the tissue lysates were prepared in potassium phosphate lysis buffer (25 mM in pH 6.5, supplemented with 0.1% (v/v) Triton X-100 and protease inhibitor 1x cocktail (Roche)) via homogenization with silent crusher S equipped with Typ 7 F/S head (30 rpm x 1000, 3 × 7 sec) on ice and lysate concentration was determined with Bicinchoninic acid (BCA) Protein Assay Kit (PierceTM).[39] The protein fractions were stored in small aliquots at -80 °C until use.

Production and Crystallisation of Recombinant GBA from BEVS

Recombinant human GBA (rhGBA) was also produced in an insect-baculovirus expression vector system (BEVS) and purified according to previously published procedures.[37] rhGBA was subsequently crystallised in a 48-well MRC sitting-drop vapour-diffusion format using previously reported 4-(2-hydroxyethyl)-1-piperazineethanesulfonic acid (HEPES) containing conditions.[37]

Co-crystal Complex with rhGBA from BEVS

Co-crystal complex of **7** was obtained by soaking unliganded rhGBA crystals (produced in BEVS) overnight in mother liquor [0.2 M sodium sulfate, 0.25 M HEPES pH 7.0, 14% (v/v) PEG 3350] spiked with 2 mM ABP **7** and 10% DMSO. Soaked crystals were transferred to a cryoprotectant solution containing 15% ethylene glycol before flash freezing in liquid nitrogen for data collection.

Data Collection, Structure Solution and Refinement

Data were collected at the i04 beamline of the Diamond Light Source (DLS) UK, and processed using XIA2[40] and AIMLESS[41,42] data reduction pipelines in the CCP4i2 suite.[43] Ligand complex of **7** with rhGBA (produced in BEVS) was solved by molecular replacement using PDB 6TJK[37] as the homologous search model.

Refinement was performed using REFMAC[44] followed by several rounds of manual model building with COOT.[45,46] Idealized coordinate sets and refinement dictionaries for the ligand were generated using JLIGAND.[47] Sugar conformations were validated using Privateer[48] and all structures were validated using MolProbity[49] and the wwPDB Validation service (validate-rcsb-1.wwpdb.org/) prior to deposition. Data collection and refinement statistics are summarized in Table 4.S1 and Table 4.S2 (Appendix). Crystal structure figures were generated in CCP4mg.[50]

***In vitro* activity of inhibitors on glycosidases measured by 4-MU substrates**

In vitro apparent IC_{50} measurements with compounds (**7**, **8**, **9** and **13**) in rhGBA and rhGAA were determined using the fluorogenic substrate methods described[22] previously at 3 h incubation time and 37°C. For *in vitro* apparent IC_{50} measurements of GBA2, 8 volumes of cell lysates (4 μg total protein/μL) containing overexpressed human GBA2 were firstly pre-incubated with 1 volume of MDW941 (100 nM final concentration, 0.5% (v/v DMSO)) for 30 min at 37°C to selectively inhibit GBA activity. Lysates were then incubated with 1 volume of compounds at various concentrations for 3 h at 37°C, before subsequent enzymatic assay for GBA2 activity as described earlier.[22,38] The substrate mixtures used for each enzyme are listed as follows: rhGBA, 3.75 mM 4-MU-β-D-glucopyranoside (Glycosynth, Warrington Cheshire, UK) at pH 5.2 (150 mM McIlvaine buffer), supplemented with 0.2% (w/v) sodium taurocholate and 0.1% (v/v) Triton X-100; GBA2, 3.75 mM 4-MU-β-D-glucopyranoside at pH 5.8; rhGAA, 3 mM 4-MU-α-D-glucopyranoside at pH 4.0. All assays were performed in duplicate sets, each with 3 technical replicates at each inhibitor concentration. DMSO concentration was kept at 0.5% - 1% (v/v) in all assays during incubation with compounds. *In vitro* apparent IC_{50} values were calculated by fitting data with [inhibitor] vs response—various slope (four parameters) function using Graphpad Prism 7.0 software. Average values and standard deviations were calculated from the two sets.

Titration of ABP 3 and ABP 7 with rhGBA

rhGBA produced in BEVS[37] was diluted to 200 nM in 150 mM McIlvaine buffer pH 5.2 (containing 0.1 % (v/v) Triton X-100 and 0.2 % (w/v) sodium taurocholate) and ABP **3** or ABP **7** were added to 150, 100, 50, 10, 1, 0.1, 0.01 or 0.001 nM in a final reaction volume of 10 µL. The reactions were incubated at 37 °C for 30 mins and then denatured with Laemmli (x3) sample buffer at 95 °C for 5 minutes. The samples were resolved by electrophoresis in 10% SDS-PAGE gels, running at 200 V for approximately 50 minutes. Wet slab gels were scanned on fluorescence using an Amersham Typhoon 5 Imager (GE Healthcare) with λ_{EX} 635 nm; λ_{EM} > 665 nm.

rhGBA Titration with ABP 3 and ABP 7

rhGBA produced in BEVS[37] was prepared at 500, 250, 100, 50, 10, 1, 0.1 and 0.01 nM in 150 mM McIlvaine buffer pH 5.2 (supplemented with 0.1 % (v/v) Triton X-100 and 0.2 % (w/v) sodium taurocholate). ABP **3** or ABP **7** were added to 150 nM final concentration and the reactions were incubated at 37 °C for 30 mins. The samples were denatured with Laemmli (x3) sample buffer at 95 °C for 5 minutes and resolved by electrophoresis in 10% SDS-PAGE gels, running at 200 V for approximately 50 minutes. Wet slab gels were scanned on fluorescence using an Amersham Typhoon 5 Imager (GE Healthcare) with λ_{EX} 635 nm; λ_{EM} > 665 nm.

Fluorescent Labeling of lysates and SDS-PAGE analysis

Mouse brain lysate (25 µg total protein per sample) was diluted with 150 mM McIlvaine buffer pH 5.2 (with 0.1 % (v/v) Triton X-100 and 0.2 % (w/v) sodium taurocholate) or pH 5.8 to a final 10 µL volume and labeled with different concentrations of ABPs **3**, **7** or **13** (diluted with McIlvaine buffer at matching pH to a final 5 µL volume) at 37 °C for 30 min. Fluorescent labeling with broad-spectrum ABP **6** was performed at 100 nM ABP concentration at 37 °C for 30 min at pH 5.2 (with 0.1 % (v/v) Triton X-100 and 0.2 % (w/v) sodium taurocholate) or pH 5.8 respectively. Samples were then denatured with 4 µL Laemmli (5x) sample buffer and heated at 98 °C for 5 minutes. Proteins were resolved by electrophoresis in 10% SDS-PAGE gels, running at a constant of 90V for 30 minutes followed by 120V for approximately 60 minutes. Wet slab gels were scanned on fluorescence using a Typhoon FLA9500 Imager (GE Healthcare) using λ_{EX} 635 nm; λ_{EM} > 665 nm and images were processed using ImageLab 5.2.1 (BioRad).

Competitive ABPP experiments

Mouse brain lysate (25 µg total protein per sample) was diluted with 150 mM McIlvaine buffer pH 5.2 (with 0.1 % (v/v) Triton X-100 and 0.2 % (w/v) sodium taurocholate) to a final 10 µL volume, pre-incubated with 2.5 µL of inhibitor (**8** or **9**) at varying concentrations at 37 °C for 60 min. Then, 2.5 µL of ABP **6** was added to a final concentration of 50 nM and the labeling reaction was incubated at 37 °C for 30 min. Additionally a negative control was also performed. 2.5 µL SDS (10 % (w/v)) was added to the 10 µL protein, boiling at 98 °C for 5 min, and incubated with ABP **6** at 37 °C for 30 min. Samples

were then denatured with 4 µL Laemmli (5x) sample buffer at 98 °C for 5 minutes, and proceeded to SDS-PAGE and fluorescent detection as described above.

***In situ* Labeling of HEK 293T cells and SDS-PAGE analysis**

Experiment was conducted based on the previously described methods.[27] The HEK293T cells which contain endogenous GBA and overexpressed GBA2 were cultured in 6-well plates and let them grow to at least 80% confluency before experiment. ABP **3**, ABP **6** and ABP **7** were diluted with DMSO into various concentrations (200x of the final concentration), and 5 µL of ABP at different concentrations were added into 1 mL fresh medium containing cells and incubated at 37°C for 24 h. After incubation, cells were washed 3 times with PBS, detached from culture dishes by scraping and lysed in 90 µL of 25 mM KPi buffer (pH 6.5 supplemented with 0.1% (v/v) Triton X-100 and protease inhibitor cocktail) by sonication. The protein concentrations were determined using BCA kit. For SDS-PAGE, each sample containing the same amount of protein (25 µg total protein) was diluted with 25 mM KPi buffer pH 6.5 (+0.1% (v/v) Triton X-100 and protease inhibitor cocktail) into a total volume of 15 µL, denatured by incubation with 4 µL Laemmli (5x) sample buffer at 98 °C for 5 minutes, and proceeded to SDS-PAGE and fluorescent detection as described above.

4.5.2 Chemical synthesis

General experimental details

All reagents were of a commercial grade and were used as received unless stated otherwise. Polymer-bound PPh_3 (100-200 mesh, 3.0 mmol/g loading) was purchased from Sigma-Aldrich. Dichloromethane (DCM), chloroform ($CHCl_3$), toluene, tetrahydrofuran (THF) and *N*,*N*-dimethylformamide (DMF) were stored over 4 Å molecular sieves, which were dried *in vacuo* before use. Triethylamine was dried over KOH and distilled before using. All reactions were performed under an argon atmosphere unless stated otherwise. Solvents used for flash column chromatography were of pro analysis quality. Reactions were monitored by analytical thin-layer chromatography (TLC) using Merck aluminum sheets pre-coated with silica gel 60 with detection by UV absorption (254 nm) and by spraying with a solution of $(NH_4)_6Mo_7O_{24}\cdot H_2O$ (25 g/L) and $(NH_4)_4Ce(SO_4)_4\cdot H_2O$ (10 g/L) in 10% sulfuric acid followed by charring at ~150 ˚C or by spraying with an aqueous solution of $KMnO_4$ (7%) and K_2CO_3 (2%) followed by charring at ~150 °C. Column chromatography was performed manually using either Baker or Screening Device silica gel 60 (0.04 - 0.063 mm) or a Biotage Isolera™ flash purification system using silica gel cartridges (Screening devices SiliaSep HP, particle size 15-40 µm, 60A) in the indicated solvents. ^{1}H NMR and ^{13}C NMR spectra were recorded on Bruker DMX-600 (600/150 MHz), Bruker AV-400 (400/101 MHz), Bruker AV-500 (500/126 MHz) and Bruker AV-850 (850/214 MHz) spectrometers in the given solvent. Chemical shifts are given in ppm relative to the chloroform residual solvent peak or tetramethylsilane (TMS) as internal standard. Coupling constants are given in Hz. All given ^{13}C spectra are proton decoupled. The following abbreviations are used to describe peak patterns

when appropriate: s (singlet), d (doublet), t (triplet), qt (quintet), m (multiplet), br (broad), Ar (aromatic), app (apparent). 2D NMR experiments (HSQC, COSY and NOESY) were carried out to assign protons and carbons of the new structures and assignation follows the general numbering shown in compound **10**. High-resolution mass spectra (HRMS) of intermediates were recorded with a LTQ Orbitrap (Thermo Finnigan) and final compounds were recorded with an apex-QE instrument (Bruker). LC/MS analysis was performed on an LCQ Advantage Max (Thermo Finnigan) ion-trap spectrometer (ESI+) coupled to a Surveyor HPLC system (Thermo Finnigan) equipped with a C18 column (Gemini, 4.6 mm x 50 mm, 3 µm particle size, Phenomenex) equipped with buffers A: H_2O, B: acetonitrile (MeCN) and C: 1% aqueous TFA, or an Agilent Technologies 1260 Infinity LCMS with a 6120 Quadrupole MS system equipped with buffers A: H_2O, B: acetonitrile (MeCN) and C: 100 mM NH_4OAc. For reversed-phase HPLC-MS purifications an Agilent Technologies 1200 series prepLCMS with a 6130 Qudropole MS system was used equipped with buffers A: 50 mM NH_4HCO_3 in H_2O and B: MeCN.

Experimental Procedures and Characterization Data of Products

Known compounds **2**[28] and **14**[35] were synthesized following procedures previously described and their spectroscopic data are in agreement with those previously reported.

Compound 10

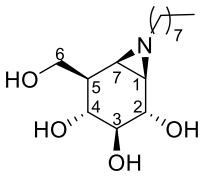

Compound **2** (475 mg, 2.71 mmol) was dissolved in anhydrous DMF (20 mL). 1-iodooctane (0.75 mL, 4.16 mmol) and K_2CO_3 (1.69 g, 12.2 mmol) were added to the solution and the mixture was stirred at 55 °C for 48 h. The reaction mixture was filtered over a pad of celite and concentrated under reduced pressure. The product was purified by silica gel column chromatography (DCM/MeOH, 100:0→90:10) affording compound **10** (300 mg, 1.05 mmol, 39%) as a yellowish oil. ^{1}H NMR (400 MHz, MeOD) δ 3.99 (dd, J = 10.1, 4.4 Hz, 1H, H6a), 3.67 – 3.56 (m, 2H, H6b and H2), 3.11 (dd, J = 9.9, 8.1 Hz, 1H, H3), 3.02 (t, J = 9.8 Hz, 1H, H4), 2.36 (dt, J = 11.7, 7.7 Hz, 1H, NCH*H*), 2.16 (dt, J = 11.5, 7.3 Hz, 1H, NCH*H*), 2.01 (dd, J = 6.4, 3.5 Hz, 1H, H7), 1.94 – 1.84 (m, 1H, H5), 1.66 (d, J = 6.3 Hz, 1H, H1), 1.63 – 1.51 (m, 2H, CH_2 octyl), 1.39 – 1.22 (m, 10H, 5CH_2 octyl), 0.93 – 0.87 (m, 3H, CH_3). ^{13}C NMR (101 MHz, MeOD) δ 79.0 (C3), 73.9 (C2), 70.1 (C4), 63.7 (C6), 62.2 (NCH_2), 45.5, 45.5 (C1 and C5), 43.1 (C7), 33.0, 30.7, 30.4, 30.3, 28.4, 23.7 (6CH_2 octyl), 14.4 (CH_3). HRMS (ESI) m/z: $[M+H]^+$ calc for $C_{15}H_{30}NO_4$ 288.21693, found 288.21674.

Compound 12

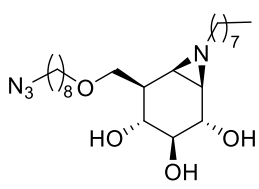

Compound **10** (16 mg, 56 µmol) was dissolved in anhydrous DCM (2 mL) and cooled to -25 °C. DIPEA (19.6 µL, 112 µmol) and freshly prepared 8-azidooctyl trifluoromethanesulfonate (1.0 M in anhydrous DCM, 112 µmol) were added, and the reaction mixture was stirred at -25 °C for 1 h and warmed to rt and stirred over-weekend. LC-MS indicated the presence of starting material so more DIPEA (19.6

µL, 112 µmol) and 8-azidooctyl trifluoromethanesulfonate (1.0 M in anhydrous DCM, 112 µmol) were added. After stirring at rt for 30 h, the reaction mixture was diluted with EtOAc, washed with sat. aq. $NaHCO_3$, water and brine, dried with anhydrous Na_2SO_4, filtered and concentrated *in vacuo*. The product was purified by silica gel column chromatography (DCM/MeOH, 100:0→90:10) affording product **12** (2.7 mg, 6.1 µmol, 11%) as a clean oil and unreacted starting material **10** (6.5 mg, 23 µmol) was recovered as well. ^{1}H NMR (600 MHz, MeOD) δ 3.80 (dd, J = 8.7, 3.9 Hz, 1H, H6a), 3.58 (d, J = 8.3 Hz, 1H, H2), 3.53 (dt, J = 9.3, 6.4 Hz, 1H, OCH*H* azido-octyl), 3.49 – 3.41 (m, 2H, H6b and OCH*H* azido-octyl), 3.28 (td, J = 6.5, 1.9 Hz, 2H, CH_2N_3), 3.10 (dd, J = 10.0, 8.3 Hz, 1H, H3), 2.97 (t, J = 9.8 Hz, 1H, H4), 2.57 (ddd, J = 11.6, 9.3, 6.5 Hz, 1H, NCH*H*), 2.03 – 1.94 (m, 2H, H5 and H7), 1.94 – 1.86 (m, 1H, NCH*H*), 1.67 (d, J = 6.2 Hz, 1H, H1), 1.64 – 1.51 (m, 6H, $3CH_2$), 1.45 – 1.24 (m, 18H, $9CH_2$), 0.91 (t, J = 7.0 Hz, 3H, CH_3). ^{13}C NMR (151 MHz, MeOD) δ 78.9 (C3), 73.8 (C2), 72.4, 72.3 (C6 and OCH_2), 69.8 (C4), 62.3 (CH_2NH_2), 52.4 (CH_2N_3), 45.8 (C1), 43.6 (C5), 43.3 (C7), 33.1, 30.9, 30.8, 30.6, 30.4, 30.3, 30.3, 30.0, 28.5, 27.8, 27.4, 23.8 ($12CH_2$), 14.5 (CH_3). HRMS (ESI) m/z: $[M+H]^+$ calc for $C_{23}H_{45}N_4O_4$ 441.34353, found 441.34388.

Compound 13

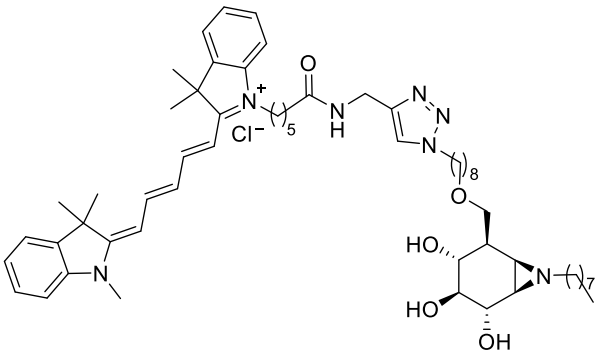

Compound **12** (2.7 mg, 6.1 µmol) was dissolved in DMF (0.5 mL). Then Cy5-alkyne (4.4 mg, 7.9 µmol), $CuSO_4$ (0.1 M in H_2O, 18.3 uL, 1.83 µmol, 0.3 eq.) and sodium ascorbate (0.1 M in H_2O, 18.3 uL, 1.83 µmol, 0.3 eq.) were added and the mixture was stirred for 24 h at rt until full conversion was observed by LC-MS. The solvent was evaporated and the product was purified by semi-preparative reversed phase HPLC (linear gradient. Solution used: A: 50 mM NH_4HCO_3 in H_2O, B: MeCN) affording ABP **13** (1.5 mg, 1.5 µmol, 25%) as a blue powder after lyophilization. ^{1}H NMR (600 MHz, MeOD) δ 8.28 (t, J = 13.0 Hz, 2H), 7.87 (s, 1H), 7.53 (d, J = 7.4 Hz, 2H), 7.45 (td, J = 7.2, 3.2 Hz, 2H), 7.32 (dt, J = 8.6, 6.7 Hz, 4H), 6.65 (t, J = 12.4 Hz, 1H), 6.31 (d, J = 13.7 Hz, 2H), 4.47 – 4.35 (m, 4H), 4.12 (t, J = 7.4 Hz, 2H), 3.82 (dd, J = 8.5, 3.9 Hz, 1H), 3.67 (s, 3H), 3.62 (d, J = 8.2 Hz, 1H), 3.55 – 3.41 (m, 3H), 3.16 – 3.08 (m, 1H), 3.00 (t, J = 9.6 Hz, 1H), 2.64 – 2.48 (m, 1H), 2.28 (t, J = 7.2 Hz, 2H), 2.04 – 1.81 (m, 10H), 1.76 (s, 14H), 1.55 (dd, J = 24.4, 7.3 Hz, 4H), 1.34 (d, J = 9.7 Hz, 18H), 0.92 (t, J = 5.6 Hz, 3H). HRMS (ESI) m/z: $[M]^+$ calc for $C_{58}H_{86}N_7O_5$ 960.66850, found 960.66832.

Compound 15

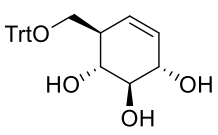

Compound **14** (1.0 g, 2.9 mmol) was dissolved in dry DCM (20 mL) and cooled to -78 °C. BCl_3 (1.0 M in DCM, 15.0 mL, 15.0 mmol) was added slowly and the mixture was stirred at -78 °C for 2 h. After quenching with MeOH, the solvent was

evaporated and the residue was co-evaporated with toluene (3 x) and directly dissolved in dry DMF (15 mL). Then Et_3N (1.0 mL, 7.5 mmol), trityl chloride (1.7 g, 6.0 mmol), and DMAP (18 mg, 0.15 mmol) were added and the reaction mixture was stirred at rt for 19 h. The mixture was diluted with H_2O, extracted with EtOAc (2 x), the combined organic layers were washed with water (2 x) and brine, dried with anhydrous Na_2SO_4, filtered and concentrated *in vacuo*. The product was purified by silica gel column chromatography (DCM/MeOH, 50:1→9:1) affording compound **15** (0.36 g, 0.89 mmol, 30% over two steps) as a pale-yellow oil. ^{1}H NMR (400 MHz, $CDCl_3$) δ 7.47 – 7.35 (m, 5H, 5CH Ar), 7.31 – 7.14 (m, 10H, 10CH Ar), 5.53 (dt, *J* = 10.1, 2.4 Hz, 1H, H7), 5.40 (dt, *J* = 10.2, 2.1 Hz, 1H, H1), 4.18 – 4.06 (m, 1H, H2), 3.61 – 3.49 (m, 2H, H3 and H4), 3.25 (dd, *J* = 8.8, 5.4 Hz, 1H, H6a), 3.21 – 3.13 (m, 1H, H6b), 2.50 – 2.42 (m, 1H, H5). ^{13}C NMR (101 MHz, $CDCl_3$) δ 143.9 ($3C_q$ Ar), 129.3 (C1), 128.7 (6CH Ar), 128.0 (6CH Ar), 127.4 (C7), 127.2 (3CH Ar), 87.1 (C_q), 77.7 (C3/C4), 72.3 (C2), 72.3 (C3/C4), 65.1 (C6), 44.4 (C5). HRMS (ESI) m/z: $[M+Na]^+$ calc for $C_{26}H_{26}O_4Na$ 425.17233, found 425.17274.

Compound 16

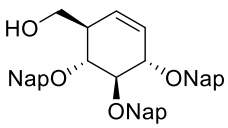

Compound **15** (328 mg, 0.815 mmol) was dissolved in dry DMF (6 mL) and cooled to 0 °C. NaH (60% in mineral, 261 mg, 6.52 mmol) was added to the mixture and stirred at 0 °C for 30 min. Then NapBr (1.08 g, 4.86 mmol) and TBAI (30 mg, 0.082 mmol) were added successively and stirred at 0 °C for 10 min. Then the mixture was warmed to rt and stirred for 5 h. The reaction was quenched with H_2O at 0 °C, diluted with H_2O and extracted with EtOAc (2 x), the combined organic layers were washed with water (2 x) and brine, dried with anhydrous Na_2SO_4, filtered and concentrated *in vacuo*. The crude was then dissolved in a mixture of DCM/MeOH (1/1, 4 mL/4mL). TsOH was added until pH ≈ 2 and the mixture was stirred at rt overnight. Et_3N was added to quench the reaction and the solvent was concentrated *in vacuo*. EtOAc was added and the solution was washed with sat. aq. NH_4Cl, sat. aq. $NaHCO_3$, H_2O and brine, dried over Na_2SO_4, filtered and concentrated *in vacuo*. The product was purified by silica gel column chromatography (pentane/EtOAc, 6:1→3:1) affording compound **16** (345 mg, 0.595 mmol, 73%) as a white solid. ^{1}H NMR (400 MHz, $CDCl_3$) δ 7.88 – 7.63 (m, 11H, 11CH Ar), 7.53 – 7.34 (m, 10H, 10CH Ar), 5.80 (dt, *J* = 10.1, 2.5 Hz, 1H, H7), 5.57 (dt, *J* = 10.1, 2.0 Hz, 1H, H1), 5.17 (d, *J* = 11.5 Hz, 1H, CH*H* Nap), 5.12 (d, *J* = 4.4 Hz, 2H, CH_2 Nap), 4.87 (s, 2H, CH_2 Nap), 4.83 (d, *J* = 11.3 Hz, 1H, CH*H* Nap), 4.35 (ddd, *J* = 7.8, 3.4, 1.9 Hz, 1H, H2), 3.96 (dd, *J* = 10.1, 7.7 Hz, 1H, H6a), 3.81 – 3.65 (m, 3H, H6b, H3 and H4), 2.59 – 2.53 (m, *J* = 9.4, 3.3 Hz, 1H, H5), 1.78 – 1.49 (br s, 1H, OH). ^{13}C NMR (101 MHz, $CDCl_3$) δ 136.4, 136.0, 135.8, 133.4, 133.4, 133.4, 133.1, 133.1, 133.0 ($9C_q$ Ar), 128.4, 128.4, 128.3, 128.3, 128.2, 128.1, 128.0, 128.0, 127.8, 127.0, 126.9, 126.7, 126.6, 126.3, 126.2, 126.2, 126.1, 126.1, 126.0, 126.0, 125.9 (21CH Ar, C1 and C7), 85.2 (C4), 80.8, 79.0 (C2 and C3), 75.4, 75.3, 72.2 ($3CH_2$ Nap), 63.4 (C6), 45.9 (C5). HRMS (ESI) m/z: $[M+NH_4]^+$ calc for $C_{40}H_{40}O_4N$ 598.29519, found 598.29479.

Compound S2

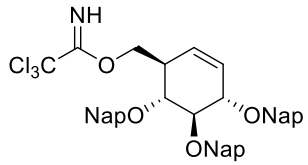

Compound **16** (0.34 g, 0.59 mmol) was dissolved in dry DCM (5.0 mL). Then trichloroacetonitrile (117 µL, 1.18 mmol) and DBU (9 µL, 59 µmol) were added and the mixture was stirred at rt overnight. The mixture was concentrated and the product was purified by silica gel column chromatography (pentane/EtOAc, 13:1→7:1) affording intermediate **S2** (302 mg) as a clean oil which was not completely pure and a yield over two steps is provided after the next step. *Note: TLC-analysis showed clean conversion of the reaction, while the product partly decomposed during a purification attempt by column chromatography, forming a less polar impurity which was eluted out together with the product.*

Compound 17

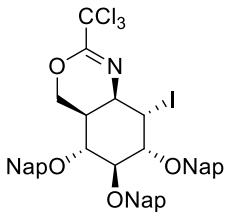

Compound **S2** (0.30 g) was co-evaporated with toluene, dissolved in dry $CHCl_3$ (4.5 mL) and cooled down to 0 °C. Then NIS (140 mg, 0.62 mmol) was added and the mixture was stirred at rt for 17 h. The reaction was quenched with sat. aq. $Na_2S_2O_3$ and stirred vigorously for 10 minutes. The mixture was diluted with $CHCl_3$, washed with sat. aq. $NaHCO_3$, H_2O and brine, dried over Na_2SO_4, filtered and concentrated *in vacuo*. The product was purified by silica gel column chromatography (pentane/EtOAc, 50:1→20:1) affording compound **17** (199 mg, 0.234 mmol, 40% over two steps) as a white solid. ^{1}H NMR (850 MHz, $CDCl_3$) δ 7.86 – 7.78 (m, 6H, 6CH Ar), 7.76 (dd, *J* = 8.1, 1.4 Hz, 1H, CH Ar), 7.74 – 7.70 (m, 3H, 3CH Ar), 7.68 (d, *J* = 1.7 Hz, 1H, CH Ar), 7.63 (dd, *J* = 7.9, 1.3 Hz, 1H, CH Ar), 7.58 (dd, *J* = 8.4, 1.7 Hz, 1H, CH Ar), 7.51 – 7.39 (m, 8H, 8CH Ar), 5.19 – 5.16 (m, 2H, CH_2 Nap), 4.98 (d, *J* = 10.7 Hz, 1H, CH*H* Nap), 4.93 (d, *J* = 11.3 Hz, 1H, CH*H* Nap), 4.85 (t, *J* = 3.4 Hz, 1H, H2), 4.80 (dd, *J* = 11.3, 4.2 Hz, 2H, CH_2 Nap), 4.66 (dd, *J* = 11.3, 1.4 Hz, 1H, H6a), 4.27 (dd, *J* = 11.2, 2.9 Hz, 1H, H6b), 4.10 – 4.06 (m, 2H, H4 and H1), 3.48 (dd, *J* = 11.2, 9.2 Hz, 1H, H7), 2.84 (dd, *J* = 9.3, 3.8 Hz, 1H, H3), 2.76 (dddd, *J* = 11.2, 4.4, 2.9, 1.4 Hz, 1H, H5). ^{13}C NMR (214 MHz, $CDCl_3$) δ 153.5 (C=N), 135.9, 135.4, 135.0, 133.4, 133.4, 133.4, 133.3, 133.2, 133.1 (9C_q Ar), 128.5, 128.5, 128.3, 128.2, 128.1, 128.1, 127.9, 127.8, 127.8, 127.5, 127.2, 127.1, 126.5, 126.5, 126.3, 126.3, 126.2, 126.2, 126.2, 126.0, 126.0 (21CH Ar), 91.4 (CCl_3), 85.2 (C4), 77.2 (C3), 76.4, 76.2 (2CH_2 Nap), 76.1 (C7), 72.4 (CH_2 Nap), 68.3 (C6), 58.7 (C1), 36.3 (C2), 33.8 (C5). HRMS (ESI) m/z: $[M+H]^+$ calc for $C_{42}H_{36}Cl_3INO_4$ 850.07491, found 850.07431.

Compound 18

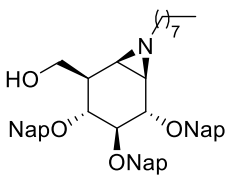

Compound **17** (0.19 g, 0.22 mmol) was dissolved in a mixture of DCM/MeOH (1/1, 1 mL/1 mL) and HCl (1.25 M in MeOH, 0.53 mL, 0.66 mmol) was added. The mixture was stirred overnight and subsequently neutralized by addition of Amberlite IRA-67. After stirring at rt for 20 h, the reaction mixture was filtered

and the resin was washed with DCM/MeOH (3 x). The filtrate was concentrated to afford an oil which was co-evaporated with toluene (3 x) and directly taken up in dry DMF (2 mL). Then K_2CO_3 (39 mg, 0.28 mmol) and 1-iodooctane (86 µL, 0.48 mmol) were added. The mixture was heated up to 80 °C and stirred for 16 h. After cooling to rt, the mixture was diluted with H_2O, extracted with EtOAc (2 x), the combined organic layers were washed with water (2 x) and brine, dried over Na_2SO_4, filtered and concentrated *in vacuo*. The product was purified by silica gel column chromatography (pentane/EtOAc, 7:1→4:1) affording compound **18** (55 mg, 78 µmol, 35% over two steps) as a pale yellow solid. ^{1}H NMR (500 MHz, $CDCl_3$) δ 7.83 – 7.69 (m, 9H, 9CH Ar), 7.69 – 7.60 (m, 3H, 3CH Ar), 7.52 – 7.35 (m, 9H, 9CH Ar), 5.15 – 4.85 (m, 5H, 5CH*H* Nap), 4.74 (d, *J* = 10.9 Hz, 1H, 1CH*H* Nap), 4.03 – 3.90 (m, 2H, H6ab), 3.90 – 3.82 (m, 1H, H2), 3.66 – 3.57 (m, 2H, H3 and H4), 2.95 – 2.80 (br s, 1H, OH), 2.23 (dt, *J* = 11.5, 7.2 Hz, 1H, NCH*H*), 2.17 – 2.06 (m, 2H, H5 and NCH*H*), 1.84 (dd, *J* = 6.3, 3.5 Hz, 1H, H7), 1.60 (d, *J* = 6.3 Hz, 1H, H1), 1.46 (p, *J* = 7.7 Hz, 2H, CH_2), 1.32 – 1.17 (m, 10H, 5CH_2), 0.89 (t, *J* = 7.0 Hz, 3H, CH_3). ^{13}C NMR (126 MHz, $CDCl_3$) δ 136.6, 136.1, 135.7, 133.5, 133.4, 133.4, 133.2, 133.1, 133.0 (9C_q Ar), 128.4, 128.2, 128.1, 128.1, 127.8, 127.8, 127.7, 126.9, 126.7, 126.4, 126.3, 126.1, 126.1, 126.1, 126.1, 125.9, 125.8 (21CH Ar), 85.6 (C3), 81.5 (C2), 77.1 (C4), 75.8, 75.4, 73.0 (3CH_2 Nap), 63.9 (C6), 61.1 (NCH_2), 43.3 (C5), 42.6 (C7), 40.7 (C1), 32.0, 29.6, 29.6, 29.4, 27.5, 22.8 (6CH_2), 14.3 (CH_3). HRMS (ESI) m/z: $[M+H]^+$ calc for $C_{48}H_{54}NO_4$ 708.40474, found 708.40436.

Compound 19

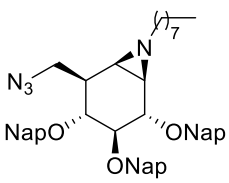

Compound **18** (50 mg, 70 µmol) was dissolved in dry DCM (0.7 mL) in a microwave tube. Et_3N (19 µL, 0.14 mmol) and *N*-methyl imidazole (40 µL, 0.50 mmol) were added and the mixture was cooled to 0 °C. Tosylchloride (40 mg, 0.21 mmol) was added at 0 °C. The tube was then sealed and the mixture was stirred at rt for 28 h. The reaction was quenched with H_2O at 0 °C, diluted with EtOAc, washed with diluted aq. 1.0 M HCl, sat. aq. $NaHCO_3$, H_2O and brine, dried over Na_2SO_4, filtered and concentrated *in vacuo*. After co-evaporation with toluene (2 x), the crude intermediate was dissolved in dry DMF (0.7 mL). NaN_3 (45 mg, 0.70 mmol) was added and the mixture was heated up to 50 °C and stirred for 40 h. After cooling to rt, the mixture was diluted with H_2O, extracted with EtOAc (2 x), the combined organic layers were washed with H_2O (2 x) and brine, dried over Na_2SO_4, filtered and concentrated *in vacuo*. The product was purified by silica gel column chromatography (pentane/EtOAc, 18:1→10:1) affording compound **19** (35 mg, 48 µmol, 68% over two steps) as a white solid. ^{1}H NMR (400 MHz, $CDCl_3$) δ 7.84 – 7.58 (m, 12H, 12CH Ar), 7.53 – 7.31 (m, 9H, 9CH Ar), 5.10 – 4.85 (m, 5H, 5CH*H* Nap), 4.60 (d, *J* = 11.2 Hz, 1H, 1CH*H* Nap), 3.89 (d, *J* = 8.2 Hz, 1H, H2), 3.76 (dd, *J* = 11.6, 3.5 Hz, 1H, H6a), 3.56 (dd, *J* = 10.0, 8.1 Hz, 1H, H3), 3.31 (dd, *J* = 11.6, 10.0 Hz, 1H, H6b), 3.23 (t, *J* = 10.0 Hz, 1H, H4), 2.22 – 2.09 (m, 3H, H5 and NCH_2), 1.88 (dd, *J* = 6.1, 3.1 Hz, 1H, H7), 1.70 (d, *J* = 6.1 Hz, 1H, H1), 1.44 (tt, *J* = 9.2, 6.9, 3.1 Hz, 2H, CH_2), 1.26 (d, *J* = 6.3 Hz, 10H, 5CH_2), 0.89 (t, *J* = 6.7 Hz, 3H, CH_3). ^{13}C NMR (101 MHz, $CDCl_3$) δ 136.5, 135.9, 135.6, 133.4, 133.4, 133.4, 133.2, 133.1, 133.0 (9C_q Ar),

128.4, 128.3, 128.1, 128.1, 128.0, 127.8, 127.8, 126.9, 126.7, 126.4, 126.3, 126.2, 126.1, 126.1, 126.1, 126.0, 126.0, 125.8 (21CH Ar), 85.7 (C3), 81.5 (C2), 77.3 (C4), 75.6, 75.4, 72.9 ($3CH_2$ Nap), 61.1 (NCH_2), 52.3 (C6), 42.3 (C5), 42.1 (C7), 42.0 (C1), 32.0, 29.6, 29.6, 29.4, 27.5, 22.8 ($6CH_2$), 14.4 (CH_3). HRMS (ESI) m/z: $[M+H]^+$ calc for $C_{48}H_{53}N_4O_3$ 733.41122, found 733.41092.

Compound 11

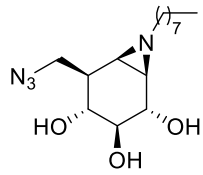

Compound **19** (31 mg, 42 µmol) was dissolved in a mixture of DCM/H_2O (10/1, 0.8 mL/0.08 mL) and DDQ (39 mg, 0.17 mmol) was added. Then the mixture was stirred at rt for 24 h until full conversion was observed by LC-MS. The reaction was quenched with a mixture of sat. aq. $NaHCO_3$ and sat. aq. $Na_2S_2O_3$, extracted with EtOAc (3 x), the combined organic layers were washed with brine, dried over Na_2SO_4, filtered and concentrated *in vacuo*. The product was purified by silica gel column chromatography (DCM/MeOH, 100:1→19:1) and by semi-preparative reversed phase HPLC (linear gradient. Solution used: A: 50 mM NH_4HCO_3 in H_2O, B: MeCN) affording compound **11** (8.7 mg, 28 µmol, 66%) as a white powder after lyophilization. ^{1}H NMR (850 MHz, MeOD) δ 3.83 (dd, J = 11.8, 3.6 Hz, 1H, H6a), 3.58 (d, J = 8.3 Hz, 1H, H2), 3.34 – 3.31 (m, 1H, H6b), 3.09 (dd, J = 10.0, 8.3 Hz, 1H, H3), 2.98 (t, J = 9.8 Hz, 1H, H4), 2.41 (ddd, J = 11.7, 8.9, 6.5 Hz, 1H, NCH*H*), 2.11 (ddd, J = 11.8, 8.8, 5.7 Hz, 1H, NCH*H*), 1.95 – 1.92 (m, 1H, H7), 1.90 (dt, J = 9.9, 3.5 Hz, 1H, H5), 1.67 (d, J = 6.2 Hz, 1H, H1), 1.60 – 1.53 (m, 2H, CH_2), 1.41 – 1.27 (m, 10H, $5CH_2$), 0.91 (t, J = 7.2 Hz, 3H, CH_3). ^{13}C NMR (214 MHz, MeOD) δ 78.9 (C3), 73.9 (C2), 69.9 (C4), 62.1 (NCH_2), 53.5 (C6), 45.8 (C1), 43.6 (C5), 43.1 (C7), 33.0, 30.7, 30.5, 30.4, 28.4, 23.7 ($6CH_2$), 14.4 (CH_3). HRMS (ESI) m/z: $[M+H]^+$ calc for $C_{15}H_{29}N_4O_3$ 313.22342, found 313.22312.

ABP 7

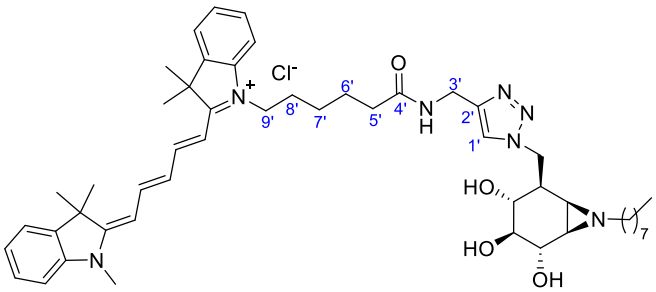

Compound **11** (4.0 mg, 13 µmol) was dissolved in DMF (0.5 mL). Then Cy5-alkyne (10.6 mg, 19 µmol), $CuSO_4$ (0.4 mg, 2.5 µmol) and sodium ascorbate (1.0 mg, 5.1 µmol) were added and the mixture was stirred overnight at rt until full conversion was observed by LC-MS. The solvent was evaporated and the product was purified by semi-preparative reversed phase HPLC (linear gradient. Solution used: A: 50 mM NH_4HCO_3 in H_2O, B: MeCN) affording ABP **7** (3.4 mg, 3.9 µmol, 30%) as a blue powder after lyophilization. ^{1}H NMR (850 MHz, MeOD) δ 8.24 (td, J = 13.0, 3.9 Hz, 2H, 2CH=CH), 7.89 (s, 1H, H1'), 7.49 (dd, J = 7.4, 1.2 Hz, 2H, 2CH Ar), 7.41 (qd, J = 7.5, 7.1, 1.2 Hz, 2H, 2CH Ar), 7.32 – 7.24 (m, 4H, 4CH Ar), 6.61 (t, J = 12.3 Hz, 1H, CH=CH), 6.28 (d, J = 13.6 Hz, 2H, 2CH=CH), 4.74 (dd, J = 13.5, 3.6 Hz, 1H, H6a), 4.51 (dd, J = 13.5, 10.0 Hz, 1H, H6b), 4.43 (s, 2H, H3'ab), 4.09 (t,

J = 7.6 Hz, 2H, H9'ab), 3.63 (s, 3H, NCH_3 Cy5), 3.59 (d, *J* = 7.8 Hz, 1H, H2), 3.15 – 3.08 (m, 2H, H4 and H3), 2.51 (ddd, *J* = 11.7, 8.4, 6.3 Hz, 1H, NCH*H* octyl), 2.28 – 2.21 (m, 3H, H5 and H5'ab), 1.87 – 1.80 (m, 3H, NCH*H* octyl and H8'ab), 1.74 – 1.68 (m, 14H, H6'ab and $4CH_3$ Cy5), 1.57 – 1.43 (m, 6H, H1, H7, H7'ab and CH_2 octyl), 1.35 – 1.23 (m, 10H, $5CH_2$ octyl), 0.88 (t, *J* = 7.1 Hz, 3H, CH_3 octyl). ^{13}C NMR (214 MHz, MeOD) *δ* 175.7, 175.5, 174.6 (C4' and C=N and *C*=CH), 155.6, 155.5 (2CH=CH), 146.4 (C2'), 144.3, 143.6, 142.6, 142.5 ($4C_q$ Ar), 129.8, 129.7, 126.6, 126.3, 126.2 (CH Ar and CH=CH), 124.6 (C1'), 123.4, 123.3, 112.0, 111.9, 104.4, 104.2 (CH Ar and CH=CH), 79.0 (C3), 74.0 (C2), 70.1 (C4), 62.1 (NCH_2 octyl), 52.0 (C6), 50.5 (C_q), 50.4 (C_q), 45.8 (C1), 44.9 (C5), 44.8 (C9'), 42.4 (C7), 36.5 (C5'), 35.7 (C3'), 33.0 (CH_2 octyl), 31.5 (NCH_3 Cy5), 30.7, 30.6, 30.4, 28.5 ($4CH_2$ octyl), 28.1 (C8'), 28.0 ($2CH_3$ Cy5), 27.8 ($2CH_3$ Cy5), 27.3 (C7'), 26.4 (C6'), 23.7 (CH_2 octyl), 14.5 (CH_3 octyl). HRMS (ESI) m/z: $[M]^+$ calc for $C_{50}H_{70}N_7O_4$ 832.54838, found 832.54775.

Compound S3

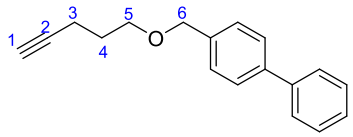

[1,1'-biphenyl]-4-ylmethanol (191 mg, 1.04 mmol) was dissolved in dry DMF (5 mL) and cooled to 0 °C. NaH (24 mg, 0.62 mmol) was added and the mixture was stirred for 10 min at 0 °C, followed by 30 min at rt. After cooling to 0 °C again, 5-bromopent-1-yne (0.10 g, 0.52 mmol) was added and the mixture was stirred at rt for 2 h. The reaction was quenched with H_2O at 0 °C and further diluted with EtOAc and H_2O. The layers were separated and the aqueous layer extracted with EtOAc. The combined organic layers were washed with H_2O (2 x) and brine, dried over Na_2SO_4, filtered and concentrated *in vacuo*. The product was purified by silica gel column chromatography (pentane/EtOAc, 100:0→100:1) affording compound **S3** (44 mg, 0.18 mmol, 35%) as a light yellow oil. ^{1}H NMR (400 MHz, $CDCl_3$) *δ* 7.62 – 7.54 (m, 4H, 4CH Ar), 7.48 – 7.38 (m, 4H, 4CH Ar), 7.38 – 7.29 (m, 1H, CH Ar), 4.55 (s, 2H, H6ab), 3.61 (t, *J* = 6.2 Hz, 2H, H5ab), 2.34 (td, *J* = 7.1, 2.7 Hz, 2H, H3ab), 1.94 (t, *J* = 2.7 Hz, 1H, H1), 1.85 (tt, *J* = 7.2, 6.2 Hz, 2H, H4ab). ^{13}C NMR (101 MHz, $CDCl_3$) *δ* 141.1, 140.7, 137.6 ($3C_q$ Ar), 128.9, 128.2, 127.4, 127.3, 127.2 (CH Ar), 84.1 (C1), 72.9 (C6), 68.9 (C5), 68.6 (C2), 28.8 (C4), 15.5 (C3). HRMS (ESI) m/z: $[M+H]^+$ calc for $C_{18}H_{19}O$ 251.14304, found 251.14282.

Compound S4

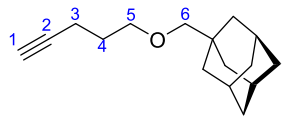

1-adamantanemethanol (173 mg, 1.04 mmol) was dissolved in dry DMF (5 mL) and cooled to 0 °C. NaH (24 mg, 0.62 mmol) was added and the mixture was stirred for 10 min at 0 °C, followed by 30 min at rt. After cooling to 0 °C again, 5-bromopent-1-yne (0.10 g, 0.52 mmol) was added and the mixture was stirred at rt for 6 h. The reaction was quenched with H_2O at 0 °C and further diluted with EtOAc and H_2O. The layers were separated and the aqueous layer extracted with EtOAc. The combined organic layers were washed with H_2O (2 x) and brine, dried over Na_2SO_4, filtered and concentrated *in vacuo*. The product was purified by silica gel column chromatography (pentane/EtOAc, 100:0→50:1) affording compound **S4** (25 mg,

0.11 mmol, 21%) as a light yellow oil. ^{1}H NMR (500 MHz, $CDCl_3$) δ 3.46 (t, J = 6.1 Hz, 2H, H5ab), 2.97 (s, 2H, H6ab), 2.29 (td, J = 7.2, 2.7 Hz, 2H, H3ab), 1.98 – 1.91 (m, 4H, H1 and 3CH), 1.81 – 1.74 (m, 2H, H4ab), 1.74 – 1.68 (m, 3H, 3CH*H*), 1.67 – 1.61 (m, 3H, 3CH*H*), 1.53 (d, J = 2.9 Hz, 6H, 6CH*H*). ^{13}C NMR (126 MHz, $CDCl_3$) δ 84.5 (C1), 82.1 (C6), 69.9 (C5), 68.3 (C2), 39.9 ($3CH_2$), 37.4 ($3CH_2$), 34.3 (C_q), 28.8 (C4), 28.5 (3CH), 15.4 (C3). HRMS (ESI) m/z: $[M+H]^+$ calc for $C_{16}H_{25}O$ 233.1899, found 233.1897.

Compound 8

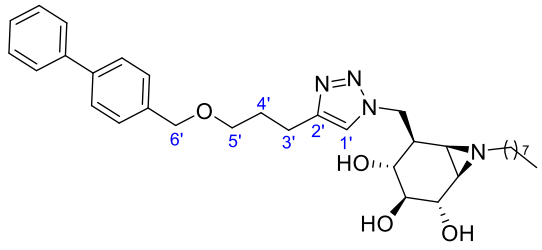

Compound **11** (2.1 mg, 6.7 µmol) was dissolved in DMF (0.3 mL) and biphenyl alkyne (2.1 mg, 8.1 µmol, dissolved with DMF, 0.1 mL in total) was added. Then $CuSO_4$ (0.1 M in H_2O, 13.4 uL, 1.34 µmol, 0.2 eq.) and sodium ascorbate (0.1 M in H_2O, 27 uL, 2.7 µmol, 0.4 eq.) were added and the mixture was stirred at rt for 16 h. Starting material was still observed by LC-MS, thus another portion of $CuSO_4$ (13.5 uL) and sodium ascorbate (27 uL) were added and the mixture was stirred for another 7 h until full conversion was observed by LC-MS. The mixture was diluted with H_2O (10 mL), extracted with EtOAc (2 x 15 mL), the combined organic layers were washed with H_2O (2 x 15 mL), brine (15 mL), dried over $MgSO_4$, filtered and concentrated in vacuo. The product was purified by silica gel column chromatography (DCM/MeOH, 100:1→20:1) affording compound **8** (3.0 mg, 5.3 µmol, 79%) as a white powder after lyophilization. ^{1}H NMR (500 MHz, $CDCl_3$) δ 7.62 – 7.55 (m, 4H, 4CH Ar), 7.46 – 7.38 (m, 4H, 4CH Ar), 7.36 – 7.32 (m, 1H, CH Ar), 7.31 – 7.29 (m, 1H, H1'), 4.59 (dd, J = 13.6, 5.3 Hz, 1H, H6a), 4.54 (s, 2H, H6'ab), 4.48 (dd, J = 13.6, 8.6 Hz, 1H, H6b), 3.97 (brs, 1H, OH), 3.83 (s, 1H, H2), 3.55 (t, J = 6.2 Hz, 2H, H5'ab), 3.44 (brs, 1H, OH), 3.36 (dd, J = 5.4, 2.2 Hz, 2H, H3 and H4), 3.27 (brs, 1H, OH), 2.84 (t, J = 7.6 Hz, 2H, H3'ab), 2.49-2.35 (m, 2H, H5 and NCH*H*), 2.06 – 1.92 (m, 3H, H4'ab and NCH*H*), 1.72 (d, J = 6.0 Hz, 1H, H1), 1.61 (dd, J = 6.0, 4.0 Hz, 1H, H7), 1.55-1.44 (m, 2H, CH_2), 1.34-1.16 (m, 10H, $5CH_2$), 0.87 (t, J = 6.5 Hz,, 3H, CH_3). ^{13}C NMR (126 MHz, $CDCl_3$) δ 147.8 (C2'), 141.0, 140.7, 137.7 ($3C_q$ Ar), 128.9, 128.4, 127.5, 127.3, 127.2 (9CH Ar), 122.0 (C1'), 76.4 (C3), 72.8 (C6'), 71.6 (C2), 69.5 (C5'), 69.3 (C4), 61.0 (NCH_2), 51.4 (C6), 43.7 (C1), 43.0 (C5), 40.5 (C7), 32.0, 29.7, 29.7, 29.5, 29.4, 27.5, 22.8, 22.5 (C4', C3' and $6CH_2$), 14.3 (CH_3). HRMS (ESI) m/z: $[M+H]^+$ calc for $C_{33}H_{47}N_4O_4$ 563.35918, found 563.35902.

Compound 9

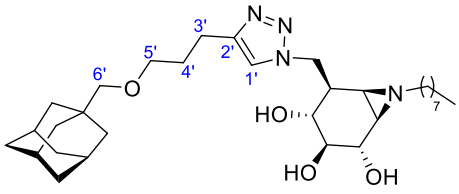

Compound **11** (2.1 mg, 6.7 µmol) was dissolved in DMF (0.3 mL) and adamantane alkyne (1.9 mg, 8.1 µmol, dissolved with DMF, 0.1 mL in total) was added. Then $CuSO_4$ (0.1 M in H_2O, 13.4 uL, 1.34 µmol, 0.2 eq.) and sodium ascorbate (0.1 M in

H_2O, 27 uL, 2.7 μmol, 0.4 eq.) were added and the mixture was stirred at rt for 16 h. Starting material was still observed by LC-MS, thus another portion of $CuSO_4$ (13.5 uL) and sodium ascorbate (27 uL) were added and the mixture was stirred for another 9 h until full conversion was observed by LC-MS. The mixture was diluted with H_2O (10 mL), extracted with EtOAc (2 x 15 mL), the combined organic layers were washed with H_2O (2 x 15 mL), brine (15 mL), dried over $MgSO_4$, filtered and concentrated in vacuo. The product was purified by silica gel column chromatography (DCM/MeOH, 100:1→20:1) and by semi-preparative reversed phase HPLC (linear gradient. Solution used: A: 50 mM NH_4HCO_3 in H_2O, B: MeCN) affording compound **9** (1.4 mg, 2.6 μmol, 39%) as a white powder after lyophilization. ^{1}H NMR (500 MHz, $CDCl_3$) δ 7.37 (s, 1H, H1'), 4.63 (dd, J = 13.6, 5.3 Hz, 1H, H6a), 4.53 (dd, J = 13.6, 8.6 Hz, 1H, H6b), 3.93 – 3.63 (m, 2H, H2 and OH), 3.45-3.38 (m, 4H, H3, H4 and H5'ab), 3.38-3.06 (brs, 2H, 2OH), 2.97 (s, 2H, H6'ab), 2.80 (t, J = 7.7 Hz, 2H, H3'ab), 2.55-2.48 (m, 1H, H5), 2.45 (dt, J = 11.5, 7.3 Hz, 1H, NCH*H* octyl), 2.05 – 1.86 (m, 4H, NCH*H* octyl and 3CH), 1.79 – 1.56 (m, 10H, H1, H7, H4'ab and 3CH_2), 1.56-1.47 (m, 8H, 4CH_2), 1.34 – 1.19 (m, 10H, 5CH_2), 0.92 – 0.85 (t, J = 5.0 Hz, 3H, CH_3). ^{13}C NMR (126 MHz, $CDCl_3$) δ 148.1 (C2'), 122.0 (C1'), 82.1 (C6'), 76.3, 71.6 (C2), 70.6 (C5'), 69.4, 61.0 (NCH_2 octyl), 51.3 (C6), 43.7 (C1), 43.0 (C5), 40.5 (C7), 39.9 (3CH_2), 37.4 (3CH_2), 34.3 (C_q), 32.0, 29.7, 29.7, 29.4, 29.4 (4CH_2 octyl and C4'), 28.4 (3CH), 27.5 (CH_2 octyl), 22.8 (C3'), 22.5 (CH_2 octyl), 14.3 (CH_3). HRMS (ESI) m/z: $[M+H]^+$ calc for $C_{31}H_{53}N_4O_4$ 545.40613, found 545.40594.

4.6 References

[1] Lombard, V.; Golaconda Ramulu, H.; Drula, E.; Coutinho, P. M.; Henrissat, B., *Nucleic Acids Res.* **2014**, *42* (D1), D490-D495.

[2] Brady, R. O.; Kanfer, J. N.; Shapiro, D., *J. Biol. Chem.* **1965**, *240*, 39–43.

[3] Beutler, E., *Science* **1992**, *256*, 794–799.

[4] Futerman, A. H.; Platt, F. M., *Mol. Genet. Metab.* **2017**, *120*, 22–26.

[5] Brady, R. O.; Kanfer, J. N.; Shapiro, D., *Biochem. Biophys. Res. Commun.* **1965**, *18*, 221–225.

[6] Brady, R. O.; Kanfer, J. N.; Bradley, R. M.; Shapiro, D., *J. Clin. Invest.* **1966**, *45*, 1112–1115.

[7] Stirnemann, J.; Belmatoug, N.; Camou, F.; Serratrice, C.; Froissart, R.; Caillaud, C.; Levade, T.; Astudillo, L.; Serratrice, J.; Brassier, A.; Rose, C.; Billette de Villemeur, T.; Berger, M., *Int. J. Mol. Sci.* **2017**, *18*, 441–470.

[8] Baris, H. N.; Cohen, I. J.; Mistry, P. K., *Pediatr Endocrinol Rev.* **2014**, *12*, 72–81.

[9] Sidransky, E., *Mol. Genet. Metab.* **2004**, *83*, 6–15.

[10] Kolodny, E. H.; Ullman, M. D.; Mankin, H. J.; Raghavan, S. S.; Topol, J.; Sullivan, J. L., *Prog. Clin. Biol. Res.* **1982**, *95*, 33–65.

[11] Erikson, A.; Bembi, B.; Schiffmann, R., *Baillieres. Clin. Haematol.* **1997**, *10*, 711–723.

[12] Nilsson, O.; Svennerholm, L., *J. Neurochem.* **1982**, *39*, 709–718.

[13] Aharon-Peretz, J.; Badarny, S.; Rosenbaum, H.; Gershoni-Baruch, R., *Neurology* **2005**, *65*, 1460–1461.

[14] Sato, C.; Morgan, A.; Lang, A. E.; Salehi-Rad, S.; Kawarai, T.; Meng, Y.; Ray, P. N.; Farrer, L. A.; St George-Hyslop, P.; Rogaeva, E., *Mov. Disord.* **2005**, *20*, 367–370.

[15] Stojkovska, I.; Krainc, D.; Mazzulli, J. R., *Cell Tissue Res.* **2018**, *373*, 51–60.

[16] Marugan, J. J.; Zheng, W.; Motabar, O.; Southall, N.; Goldin, E.; Westbroek, W.; Stubblefield, B. K.; Sidransky, E.; Aungst, R. A.; Lea, W. A.; Simeonov, A.; Leister, W.; Austin, C. P., *J. Med. Chem.* **2011**, *54*, 1033–1058.

[17] Hill, T.; M. Tropak, B.; Mahuran, D.; Withers, S. G., *ChemBioChem* **2011**, *12*, 2151–2154.

[18] Goddard-Borger, E. D.; Tropak, M. B.; Yonekawa, S.; Tysoe, C.; Mahuran, D. J.; Withers, S. G., *J. Med. Chem.* **2012**, *55*, 2737–2745.

[19] Martínez-Bailén, M.; Carmona, A. T.; Patterson-Orazem, A. C.; Lieberman, R. L.; Ide, D.; Kubo, M.; Kato, A.; Robina, I.; Moreno-Vargas, A. J., *Bioorg. Chem.* **2019**, *86*, 652–664.

[20] Street, I. P.; Kempton, J. B.; Withers, S. G., *Biochemistry* **1992**, *31*, 9970–9978.

[21] Schröder, S. P.; Wu, L.; Artola, M.; Hansen, T.; Offen, W. A.; Ferraz, M. J.; Li, K.-Y.; Aerts, J. M. F. G.; Van Der Marel, G. A.; Codée, J. D. C.; Davies, G. J.; Overkleeft, H. S., *J. Am. Chem. Soc.* **2018**, *140*, 5045–5048.

[22] Artola, M.; Kuo, C.-L.; Lelieveld, L. T.; Rowland, R. J.; van der Marel, G. A.; Codée, J. D. C.; Boot, R. G.; Davies, G. J.; Aerts, J. M. F. G.; Overkleeft, H. S., *J. Am. Chem. Soc.* **2019**, *141*, 4214–4218.

[23] Witte, M. D.; Kallemeijn, W. W.; Aten, J.; Li, K.-Y.; Strijland, A.; Donker-Koopman, W. E.; van den Nieuwendijk, A. M.; Bleijlevens, B.; Kramer, G.; Florea, B. I.; Hooibrink, B.; Hollak, C. E.; Ottenhoff, R.; Boot, R. G.; van der Marel, G. A.; Overkleeft, H. S.; Aert, J. M. F. G., *Nat Chem Biol* **2010**, *6*, 907–913.

[24] Kallemeijn, W. W.; Li, K.-Y.; Witte, M. D.; A. Marques, R. A.; Aten, J.; Scheij, S.; Jiang, J.; Willems, L. I.; Voorn-Brouwer, T. M.; van Roomen, C. P. A. A.; Ottenhoff, R.; Boot, R. G.; van den Elst, H.; Walvoort, M. T. C.; Florea, B. I.; Codée, J. D. C.; van der Marel, G. A.; Aerts, J. M. F. G.; Overkleeft, H. S., *Angew. Chem. Int. Ed.* **2012**, *51*, 12529–12533.

[25] Jiang, J.; Beenakker, T. J. M.; Kallemeijn, W. W.; van der Marel, G. A.; van den Elst, H.; Codée, J. D. C.; Aerts, J. M. F. G.; Overkleeft, H. S., *Chem. - A Eur. J.* **2015**, *21*, 10861–10869.

[26] Withers, S. G.; Umezawa, K., *Biochem. Biophys. Res. Commun.* **1991**, *177*, 532–537.

[27] Kuo, C.-L.; van Meel, E.; Kytidou, K.; Kallemeijn, W. W.; Witte, M.; Overkleeft, H. S.; Artola, M.; Aerts, J. M. F. G., *Methods Enzymol.* **2018**, *598*, 217–235.

[28] Li, K.-Y.; Jiang, J.; Witte, M. D.; Kallemeijn, W. W.; Donker-Koopman, W. E.; Boot, R. G.; Aerts, J. M. F. G.; Codée, J. D. C.; van der Marel, G. A.; Overkleeft, H. S., *Org. Biomol. Chem.* **2014**, *12*, 7786–7791.

[29] Butters, T. D.; Dwek, R. A.; Platt, F. M., *Curr. Top. Med. Chem.* **2003**, *3*, 561–574.

[30] Wennekes, T.; van den Berg, R. J. B. H. N.; Boot, R. G.; van der Marel, G. A.; Overkleeft, H. S.; Aerts, J. M. F. G., *Angew. Chem., Int. Ed.* **2009**, *48*, 8848–8869.

[31] Cordero, F. M.; Bonanno, P.; Chioccioli, M.; Gratteri, P.; Robina, I.; Vargas, A. J. M.; Brandi, A., *Tetrahedron* **2011**, *67*, 9555–9564.

[32] Sorrentino, E.; Connon, S. J., *Org. Lett.* **2016**, *18*, 5204−5207.

[33] Aliouane, L.; Chao, S.; Brizuela, L.; Pfund, E.; Cuvillier, O.; Jean, L.; Renard, P.-Y.; Lequeux, T., *Bioorg. Med. Chem.* **2014**, *22*, 4955–4960.

[34] Gundorph Hansen, F.; Bundgaard, E.; Madsen, R., *Biochem. Biophys. Res. Commun.* **1990**, *43*, 10139–10142.

[35] Li, K.-Y.; Jiang, J.; Witte, M. D.; Kallemeijn, W. W.; Van Den Elst, H.; Wong, C. S.; Chander, S. D.; Hoogendoorn, S.; Beenakker, T. J. M.; Codée, J. D. C.; Aerts, J. M. F. G.; Van Der Marel, G. A.; Overkleeft, H. S., *Eur. J. Org. Chem.* **2014**, *2014*, 6030–6043.

[36] Dvir, H.; Harel, M.; McCarthy, A. A.; Toker, L.; Silman, I.; Futerman, A. H.; Sussman, J. L., *EMBO Rep.* **2003**, *4*, 704–709.

[37] Rowland, R. J.; Wu, L.; Liu, F.; Davies, G. J., *Acta Crystallogr. Sect. D Struct. Biol.* **2020**, *76*, 565–580.

[38] Lahav, D.; Liu, B.; Van Den Berg, R. J. B. H. N.; Van Den Nieuwendijk, A. M. C. H.; T. Wennekes,; Ghisaidoobe, A. T.; Breen, I.; Ferraz, M. J.; Kuo, C.-L.; Wu, L.; Geurink, P. P.; Ovaa, H.; Van Der Marel, G. A.; Van Der Stelt, M.; Boot, R. G.; Davies, G. J.; Aerts, J. M. F. G.; Overkleeft, H. S., *J. Am. Chem. Soc.* **2017**, *139*, 14192–14197.

[39] Smith, P. K.; Krohn, R. I.; Hermanson, G. T.; Mallia, A. K.; Gartner, F. H.; Provenzano, M. D.; Fujimoto, E. K.; Goeke, N. M.; Olson, B. J.; Klenk, D. C., *Anal. Biochem.* **1985**, *150*, 76–85.

[40] Winter, G., *J. Appl. Crystallogr.* **2010**, *43*, 186–190.

[41] Evans, P., *Acta Crystallogr. Sect. D Biol. Crystallogr.* **2006**, *62*, 72–82.

[42] Evans, P. R.; Murshudov, G. N., *Acta Crystallogr. Sect. D Biol. Crystallogr.* **2013**, *69*, 1204–1214.

[43] Winn, M. D.; Ballard, C. C.; Cowtan, K. D.; Dodson, E. J.; Emsley, P.; Evans, P. R.; Keegan, R. M.; Krissinel, E. B.; Leslie, A. G. W.; McCoy, A.; McNicholas, S. J.; Murshudov, G. N.; Pannu, N. S.; Potterton, E. A.; Powell, H. R.; Read, R. J.; Vagin, A.; Wilson, K. S., *Acta Crystallogr. Sect. D Biol. Crystallogr.* **2011**, *67*, 235–242.

[44] Murshudov, G. N.; Vagin, A. A.; Dodson, E. J., *Acta Crystallogr. Sect. D Biol. Crystallogr.* **1997**, *53*, 240–255.

[45] Emsley, P.; Cowtan, K., *Acta Crystallogr D* **2004**, *60*, 2126–2132.

[46] Emsley, P.; Lohkamp, B.; Scott, W. G.; Cowtan, K., *Acta Crystallogr. Sect. D Biol. Crystallogr.* **2010**, *66*, 486–501.

[47] Lebedev, A. A.; Young, P.; Isupov, M. N.; Moroz, O. V.; Vagin, A. A.; Murshudov, G. N., *Acta Crystallogr. Sect. D Biol. Crystallogr.* **2012**, *68*, 431–440.

[48] Agirre, J.; Iglesias-Fernández, J.; Rovira, C.; Davies, G. J.; Wilson, K. S.; Cowtan, K. D., *Nat. Struct. Mol. Biol.* **2015**, *22*, 833–834.

[49] Chen, V. B.; Arendall, W. B.; Headd, J. J.; Keedy, D. A.; Immormino, R. M.; Kapral, G. J.; Murray, L. W.; Richardson, J. S.; Richardson, D. C., *Acta Crystallogr. Sect. D Biol. Crystallogr.* **2010**, *66*, 12–21.

[50] McNicholas, S.; Potterton, E.; Wilson, K. S.; Noble, M. E. M., *Acta Crystallogr. Sect. D Biol. Crystallogr.* **2011**, *67*, 386–394.

APPENDIX

Table 4.S1. Data collection and Processing

Compound	ABP **7**
PDB Entry	6Z3I
Diffraction source	Diamond Beamline i04
Wavelength (Å)	0.979507
Temperature (K)	100
Detector	Eiger2 XE 16M
Rotation range per image (°)	0.1
Total rotation range (°)	360
Space group	P 2_1
a, *b*, *c* (Å)	53.1, 76.7, 68.0
α, β, γ (°)	90, 102, 90
Resolution range (Å)	88.49-1.80 (1.84-1.80)
Total No. of reflections	348887 (20199)
No. of unique reflections	49541 (2966)
Completeness (%)	100 (100)
Redundancy	7.0 (6.8)
$\langle I/\sigma(I) \rangle$	6.7 (0.8)
$R_{meas.}$	0.22 (2.55)
$CC_{1/2}$	0.99 (0.50)
Overall *B* factor from Wilson plot ($Å^2$)	27

Table 4.S2. Structure solution and refinement

Compound	ABP **7**
PDB Entry	6Z3I
Resolution range (Å)	88.49-1.80 (1.84-1.80)
Completeness (%)	100 (100)
No. of reflections	49519
working set	
No. of reflections	2509
test set	
Final R_{cryst}	0.19
Final R_{free}	0.20
No. of non-H atoms	
Protein	3972
Ligand	193
Water	340
Total	4505
R.m.s. deviations	
Bonds (Å)	0.013
Angles (°)	1.70
Average *B* factors (Å^2)	
Protein	26
Ligand	48
Water	36
Ramachandran plot	
Most favoured (%)	94.7
Allowed (%)	4.2